

JUL 12 1957

CONFIDENTIAL

Copy
RM L57E24a

NACA RM L57E24a

NACA

RESEARCH MEMORANDUM

CLASSIFICATION CHANGE

To Unclassified
By authority of NASA Memo dtd 52-73/5/by H. Maines
Changed by M. Ruda Date 6-11-83

SOME FACTORS AFFECTING THE STATIC LONGITUDINAL AND
DIRECTIONAL STABILITY CHARACTERISTICS OF
SUPERSONIC AIRCRAFT CONFIGURATIONS

By M. Leroy Spearman

Langley Aeronautical Laboratory
Langley Field, Va.

CLASSIFIED DOCUMENT

This material contains information affecting the National Defense of the United States within the meaning of the espionage laws, Title 18, U.S.C., Secs. 793 and 794, the transmission or revelation of which in any manner to an unauthorized person is prohibited by law.

NATIONAL ADVISORY COMMITTEE
FOR AERONAUTICS

WASHINGTON

July 12, 1957

CONFIDENTIAL

UNCLASSIFIED

NACA RM L57E24a

NATIONAL ADVISORY COMMITTEE FOR AERONAUTICS

RESEARCH MEMORANDUM

SOME FACTORS AFFECTING THE STATIC LONGITUDINAL AND
DIRECTIONAL STABILITY CHARACTERISTICS OF
SUPERSONIC AIRCRAFT CONFIGURATIONS

By M. Leroy Spearman

SUMMARY

A survey is made of the problems introduced by the increased longitudinal stability and the reduced directional stability of aircraft operating in the low supersonic speed range. The longitudinal stability increases markedly at supersonic speeds and results in high drags due to trimming and in limited control for maneuvering. The large untrimmed pitching moments can be reduced and the control requirements alleviated to some extent through the use of fuselage camber. The use of canard configurations offers some promise of reducing the drag due to trimming and increasing the controllability.

The directional stability generally deteriorates rapidly at supersonic speeds because of the reduction in vertical-tail lift-curve slope coupled with the large unstable yawing moment of the fuselage. The vertical-tail contribution is shown to be affected by many factors including the wing position, the fuselage shape, and the horizontal-tail position. The directional stability can be increased, particularly at high angles of attack, by such devices as ventral fins and forebody strakes. In addition, indications are that the directional stability might be improved through modifications to the fuselage afterbody.

INTRODUCTION

Aircraft advancing from subsonic to low supersonic speeds frequently encounter performance and control problems as a result of significant changes in static stability characteristics. These changes, which are usually evident as increased longitudinal stability and reduced directional stability, are a result of various changes in the aerodynamic characteristics of the lifting surfaces and of changes in the aerodynamic interference effects between various components that occur with increasing Mach number. Changes in the aerodynamic characteristics of lifting

UNCLASSIFIED

surfaces with Mach number might be reduced through the use of thin sections and low-aspect-ratio plan forms. The changes in interference effects, and to some extent the effects of the lifting-surface aerodynamic changes, might be offset through changes in the aircraft design.

Some effects of aircraft configuration on the stability characteristics at supersonic speeds have been presented in reference 1. This paper provides a summary of some current thoughts and studies on the causes of, and possible corrections for, the static longitudinal and directional stability and control problems of supersonic aircraft configurations. The discussion is based primarily on results obtained in the Langley 4- by 4-foot supersonic pressure tunnel for Mach numbers from 1.41 to 2.01, although some limited results are given for high subsonic speeds, and the supersonic Mach number range for one configuration extends from 1.41 to 4.65.

SYMBOLS

The longitudinal stability characteristics are referred to the wind-axis system whereas the lateral stability characteristics are referred to the body-axis system. The symbols are defined as follows:

b_V	vertical-tail span
C_D	drag coefficient
C_L	lift coefficient
C_m	pitching-moment coefficient
C_n	yawing-moment coefficient
C_p	pressure coefficient, $\frac{p - p_\infty}{q_\infty}$
c_V	vertical-tail chord at any station
\bar{c}_V	mean vertical-tail chord
c_y	section lateral-force coefficient
$C_{m,0}$	pitching-moment coefficient at zero lift
C_{L_α}	lift-curve slope

C_{l_β}	effective dihedral parameter
C_{n_β}	directional stability parameter
C_{Y_β}	lateral-force parameter
$(C_{Y_\beta})_V$	increment of C_{Y_β} provided by vertical tail
d	fuselage diameter
L/D	lift-drag ratio
M	Mach number
p	local static pressure
p_∞	free-stream static pressure
q_∞	free-stream dynamic pressure
x	longitudinal distance along vertical tail
z	vertical distance along vertical tail
z_w	wing height
α	angle of attack
β	angle of sideslip
δ_H	horizontal-tail deflection, positive with trailing edge down
δ_c	canard deflection, positive with trailing edge down
δ_e	elevator deflection, positive with trailing edge down
δ_n	fuselage-forebody deflection
η_V	vertical-tail factor, $\frac{(C_{Y_\beta})_{WBV} - (C_{Y_\beta})_{WB}}{(C_{Y_\beta})_{BV} - (C_{Y_\beta})_B}$
$\partial C_m / \partial C_L$	longitudinal stability parameter

Components and Subscripts

B	fuselage (body)
H	horizontal tail
W	wing
V	vertical tail
max	maximum
min	minimum

DISCUSSION

Longitudinal Stability

The primary problem of longitudinal stability for supersonic aircraft configurations is the increased stability which occurs through the transonic range and the resultant large static margins at lower supersonic speeds. This increased stability, as pointed out in reference 1, usually results from the combined effects of a rearward shift in the center of pressure of the wing, the loss of wing downwash at the tail, and the stabilizing influence of the wing lift carried over to the fuselage afterbody. Although this increased stability is not a dangerous condition, it can result in serious limitations to the aircraft performance. These limitations arise from the fact that the excessive static margins occurring at low supersonic speeds result in large pitching moments that must be trimmed through large deflections of the pitch control and this effect, of course, results in increased trim drag. Moreover, for tail-rearward designs (designs with controls behind the center of gravity), the control deflections required for trimming produce substantial negative increments of lift. Thus, in order to trim at a given lift, a higher angle of attack with an attendant drag increase is required and the result is generally a marked reduction in L/D due to trimming. In addition, if large deflections of the control are required for trimming, the amount of control deflection available for maneuvering will be small.

The primary factors that govern the magnitude of the pitching moment to be trimmed at a given lift are the pitching-moment coefficient at zero lift $C_{m,0}$ and the slope of the pitching-moment curve $\partial C_m / \partial C_L$. Desirable design characteristics at low supersonic speeds would be those that increase the positive value of $C_{m,0}$ or decrease the negative slope of $\partial C_m / \partial C_L$, inasmuch as these characteristics would tend to reduce the control deflections required for trimming. Some of the factors that affect $C_{m,0}$ and $\partial C_m / \partial C_L$ are discussed in the subsequent sections.

Effects of fuselage camber.- One means of varying $C_{m,0}$ for a basic configuration is through the use of fuselage camber. Such a plan has been discussed in reference 1, and the effects of fuselage camber for a 60° delta-wing-fuselage combination at $M = 1.61$ are presented in reference 2. These results, which are reproduced in figure 1, indicate that the cambered fuselage produces a constant pitching-moment increment throughout the lift range with no significant increase in drag and hence should be useful in alleviating the pitch-control requirements and the attendant drag due to trimming. Results obtained in the Langley 8-foot transonic tunnel at high subsonic and transonic speeds for the configurations shown in figure 1 indicate essentially the same increment of $C_{m,0}$ as that obtained at $M = 1.61$ although the static margin is lower. This fact should be considered in assessing the merits of fixed fuselage camber.

Another form of the cambered fuselage effect can be realized through the use of a deflected forebody which has the advantage of being adjustable in flight. The effects of deflecting the forebody of a 45° swept-wing-fuselage combination at $M = 2.01$ are shown in figure 2. Deflections of the forebody provide progressive shifts in C_m similar to that provided by conventional pitch controls but without any increase in drag. Although the deflections shown are opposite to those required for trimming at positive lifts, upward deflections of the nose would be expected to provide positive increments of $C_{m,0}$.

Effect of vertical location of horizontal tail.- The vertical location of the horizontal tail has a significant effect on the longitudinal stability and control characteristics. A primary consideration at subsonic speeds is the location of the tail with respect to the wing downwash field. Generally it is advantageous, particularly for swept-wing configurations, to place the tail on or below the extended chord plane of the wing in order to avoid the regions of high downwash variation with angle of attack that lead to pitch-up. Unfortunately, these low-tail positions usually aggravate the problem of excessive longitudinal stability at supersonic speeds, inasmuch as the tail may encounter a field of upwash from the fuselage. (See refs. 3 to 5, for example.)

High horizontal tails, on the other hand, have some beneficial effects at supersonic speeds. As shown in reference 3, for example, substantial increases in trim lift were obtained through the positive shifts in $C_{m,0}$ provided by a relatively high-tail configuration at $M = 2.01$. However, such tail positions would probably cause undesirable pitch-up tendencies at subsonic and low supersonic speeds.

Some effects of Mach number on $C_{m,0}$ and $\partial C_m / \partial C_L$ for a 45° sweptback-wing and tail configuration are shown in figure 3. These results indicate rather large changes for the high horizontal tails and relatively

small changes for the low horizontal tails. With the highest tail, for example, values of both $C_{m,0}$ and $\partial C_m / \partial C_L$ decrease with increasing Mach number (a similar effect was noted in ref. 6 for a high-tail configuration). For the second highest tail, however, $C_{m,0}$ increases and $\partial C_m / \partial C_L$ decreases with Mach number (fig. 3). Similar results were obtained with a high wing and with the wing removed. Although certain combinations of $C_{m,0}$ and $\partial C_m / \partial C_L$ may result in improved performance at a given Mach number, the large variation in these quantities with Mach number may lead to some undesirable characteristics. In particular, the variation of control deflection for trim with Mach number may be undesirably nonlinear.

The variation in C_m with horizontal-tail position at supersonic speeds appears to be related to the vertical-tail induced flow-field effects on the horizontal tail. Notice, for example, the difference in the increment of $C_{m,0}$ provided by the tails just above and just below the body even though these tails are located symmetrically with respect to the body (fig. 3). The flow-field effects are sensitive to the location of the horizontal tail with respect to the vertical tail and would be expected to change with Mach number as well as with vertical-tail plan form and section.

Some effects of the modifications of the vertical-tail plan form on the pitching-moment characteristics for the high-tail configuration (fig. 3) are shown in figure 4 with the wing removed. These modifications, which were designed to relocate the leading edge of the vertical tail, had a pronounced effect on C_m and on the variation of $C_{m,0}$ with β .

Effects of auxiliary canard surfaces.- Perhaps the most frequently suggested means for reducing the stability level at supersonic speeds is the use of auxiliary canard surfaces in conjunction with a conventional horizontal-tail pitch control. Such surfaces, of course, provide a destabilizing moment which reduces the pitch-control requirements. In addition, the canard surface may be deflected to provide additional pitch control. Results for a 40° sweptback-wing airplane at $M = 1.89$ with an auxiliary canard surface are reported in reference 7 and some results are shown in figure 5. The addition of the canard at zero deflection provides a substantial reduction in stability and an increase in trim C_L . With the canard deflected 10° , an additional increase in trim C_L was obtained.

The use of auxiliary canard surfaces would also reduce the stability at subsonic speeds so that at these speeds it may be necessary to retract the canard surface, allow it to float freely, or be controlled by a servo-control system such that it acts as a free-floating surface.

Characteristics of basic canard-type configuration.- Another approach to the longitudinal stability problem is through the use of a basic canard-type configuration rather than auxiliary canard surfaces added to a conventional configuration. The stability and control characteristics of two such basic canard configurations at $M = 1.41$ and 2.01 are presented in reference 8. The purpose of the basic canard configuration would be not only to reduce the stability level at supersonic speeds but also to reduce the longitudinal stability increase that occurs in going from subsonic speeds to supersonic speeds. This reduction in stability through the transonic range is partially accomplished through the elimination of the afterbody and the conventional rearward horizontal tail so that the lift carry-over effects of the wing on the afterbody and the downwash changes at the tail are avoided. Thus, inasmuch as the static margin may be kept small because it is essentially invariant with Mach number, the control deflections required for trimming may be kept small. The control effectiveness of canard surfaces may benefit through the use of a long moment arm with only small deflections and lifts required so that the wake effects and drag from the canard surfaces would be minimized. The use of a long moment arm is compatible with the current trend toward large bodies of high fineness ratio. In addition, other problems that are associated with the wing downwash effects or jet-exhaust effects on rearward tails might be avoided through the use of canard configurations.

A comparison of the variation of the static longitudinal stability parameter $\partial C_m / \partial C_L$ with Mach number for a sweptback-wing tail-rearward configuration and a 60° delta-wing canard configuration (ref. 8) is shown in figure 6. Because of the elimination of the conventional afterbody and tail, the change in the level of stability from subsonic to supersonic speeds is considerably less for the delta-wing canard configuration than for the sweptback-wing tail-rearward configuration. Thus, the stability parameter for the canard configuration could be safely reduced to a low level in order to reduce the pitch-control requirements, whereas the stability parameter for the tail-rearward arrangement could only be reduced about 0.05 before neutral stability would be encountered at subsonic speeds.

The use of canard configurations at low speeds may provide some problems such as that of trimming to maximum lift. However, the results of low-speed studies (such as those reported in refs. 9 and 10) indicate that these problems are not insurmountable.

Comparison of canard and tailless configurations.- The stability change with Mach number can also be minimized through the use of delta-wing tailless configurations. However, tailless configurations may still experience trim and control deficiencies because of the inherently short moment arm for the control surfaces.

A comparison of the longitudinal trim characteristics for a tailless configuration and a canard delta-wing configuration (ref. 8) at a Mach number of 2.01 is shown in figure 7. The value of $\partial C_m / \partial C_L$ for both configurations was -0.15. The results indicate a considerably higher maximum trim lift for the canard configuration that could be reflected in significant performance gains. For example, with an assumed wing loading of 100 pounds per square foot, the maximum trim lifts obtained would permit level flight at 70,000 feet for the canard configuration, as compared with level flight at 48,000 feet for the tailless aircraft. In addition, the higher maximum trim lift available would result in greater maneuverability for the canard configuration than for the tailless configuration.

The canard configuration indicates higher trimmed values of L/D than those obtained for the tailless configuration although the comparison of L/D for the two configurations is affected by the difference in minimum drag. However, with the drag for the tailless aircraft adjusted to the same minimum value as for the canard aircraft, the maximum trimmed value of L/D for the tailless aircraft would be about 4.3 compared to 5.6 for the canard configuration.

A comparison of the trimmed and untrimmed (δ_c or $\delta_e = 0$) results for the tailless and canard configurations is shown in figure 8. The primary effect of trimming is apparent in the lift-curve slopes. The canard control has essentially no effect on the lift curve inasmuch as the positive lift increments from the canard are offset by slight losses in wing lift. On the other hand, deflection of the trailing-edge flap control for the tailless configuration causes a reduction in lift-curve slope. Thus, in order to maintain a constant lift in trim, the tailless configuration must operate at a higher angle of attack and, hence, at a higher drag.

Longitudinal-stability characteristics of canard configuration over wide Mach number range.- The longitudinal-stability characteristics throughout a large Mach number range for a canard airplane with an unswept-tapered wing are shown in figure 9. These results were obtained from tests of one model in the Langley high-speed 7- by 10-foot tunnel, the Langley 4- by 4-foot supersonic pressure tunnel (ref. 8), and the Langley Unitary Plan wind tunnel. The results indicate a moderate increase in longitudinal stability from subsonic to supersonic speeds that is somewhat greater than that indicated by the delta-wing canard airplane (fig. 6) but is still less than the increase generally experienced by tail-rearward aircraft.

A transonic drag-rise factor of approximately 2 is indicated and relatively low minimum drag values were obtained in the supersonic range. The maximum trimmed values of L/D vary from about 4.5 at $M = 1.41$ to 5.8 at $M = 4.65$. Relatively little loss in L/D due to trimming is

indicated, particularly at the higher Mach numbers where the stability level is lowest. The stability parameter $\partial C_m / \partial C_L$ for this configuration could be safely reduced by at least 0.10 so that the trimmed values of L/D would approach the untrimmed values.

Directional Stability

The directional stability parameter $C_{n\beta}$, as pointed out in reference 1, is characterized by a rapid decrease with increasing supersonic speed. The primary aerodynamic effect involved is the lift-curve slope of the vertical tail which begins to decrease with increasing supersonic Mach number, whereas the forces and moments on the fuselage remain essentially constant. The fundamental problem in maintaining adequate static directional stability for many current designs is in the large unstable yawing moment of the fuselage that must be overcome by the tail. These large unstable moments generally result from the use of large fuselages with high-fineness ratio and far rearward center-of-gravity positions. Such fuselage shapes are usually required to provide the volume necessary to store the equipment and fuel and still provide a low-drag profile. The far rearward center-of-gravity positions occur because it is necessary to locate large jet engines in the rear of the fuselage. The trend in fuselage design is illustrated in figure 10 wherein three single-place, single-engine fighter airplanes ranging from the World War II period to the time of the publication of this report are compared. These designs are drawn to the same scale and are aligned with their centers of gravity in the same plane. The large increase in fuselage length forward of the center of gravity is apparent. The tail length has not changed greatly although the size of the vertical tail has increased considerably.

Because of these changes in fuselage shape, a considerable portion of the vertical-tail contribution to directional stability is required to overcome the fuselage instability, while a proportionately smaller amount of the tail contribution is available to provide a positive margin of stability. Hence, any loss in tail contribution arising from such factors as decreasing tail lift-curve slope, aeroelasticity, wing-fuselage wake, interference flow fields, or forebody vorticity would subtract directly from the stability margin.

Thus, with an initially low level of directional stability at low angles of attack, many current supersonic designs become particularly sensitive to angle-of-attack changes since with increasing angle of attack the induced wake and vorticity effects appear in the wing and fuselage flow fields. (See, for example, refs. 11 to 13.)

Estimated vertical-tail contribution at $\alpha = 0^\circ$.- The accurate prediction of the vertical-tail contribution to directional stability is

difficult because of the many factors that affect the flow at the tail. A correlation of estimated and experimental values of the vertical-tail contribution to lateral force $(C_{Y\beta})_V$ at $\alpha = 0^\circ$ is shown in figure 11.

These results were obtained for a number of models tested in the Langley 4- by 4-foot supersonic pressure tunnel in the Mach number range from 1.4 to 2. The estimated values were obtained by, first, determining the lift-curve slope for the exposed portion of the vertical tail in a uniform free-stream flow field with the assumption that the body forms a perfect end plate. Then a factor was applied to this slope by the method of reference 14 to account for the lift carry over between the tail and the body. Although this method of estimating the tail contribution is arbitrary, the results indicate a fairly even scatter about the line of perfect agreement. The scatter is quite large, however, and indicates differences between the estimated and experimental values thus far obtained as large as 20 to 25 percent. These differences are a result of changes in the flow field that are induced by such things as the body, wing, and horizontal tail and are not accounted for in the estimated values. Some of these factors that affect the flow field are discussed in the following sections.

Effect of wing position.- Some effects of the body and wing on the vertical-tail contribution to $C_{Y\beta}$ and $C_{n\beta}$ are shown in figure 12 for a 45° sweptback-wing model at $M = 1.41$ and 2.01 . With the wing off, the vertical-tail contribution to $C_{Y\beta}$ and $C_{n\beta}$ (difference between tail-on

and tail-off curves) decreases with increasing angle of attack because of the sidewash induced by body vorticity. As pointed out in reference 1, the addition of a high wing to a circular body causes an additional sidewash distribution in the wing wake that is adverse above the center of the wing wake and favorable below. The addition of a low wing, on the other hand, causes an additional sidewash distribution that is favorable above and adverse below the center of the wing wake. Thus, at $\alpha = 0^\circ$, the contribution of the vertical tail to $C_{Y\beta}$ and $C_{n\beta}$ is decreased by

the addition of the high wing and increased by the addition of the low wing (fig. 12). As the angle of attack is increased, the afterbody and vertical tail must move down through the wing-induced sidewash fields with the result (see fig. 12) that, for the high-wing arrangement, the tail contribution decreases while the wing-body becomes less unstable, whereas for the low-wing arrangement, the tail contribution is essentially constant but the wing-body configuration becomes more unstable. The directional stability for the complete model decreases with increasing angle of attack in both cases, however, because of the decreased tail contribution for the high-wing configuration and because of an increase in the instability of the wing-body model for the low-wing configuration.

In addition to the expected difference in the level of $C_{n\beta}$ and $C_{Y\beta}$ between $M = 1.41$ and 2.01 (fig. 12), the effects of wing position appear

to be less at the higher Mach number. There are several factors that may contribute to this lessening of the effects of wing position. For one thing, because of the decreased wing lift-curve slope at the higher Mach number, the strength of the wing-body induced vortex flow and the resultant sidewash angle at the tail may be reduced. A decrease in wing-position effects might also result from the decreased tail lift-curve slope which, even for a constant sidewash angle at the tail, would result in a smaller incremental change in vertical-tail contribution.

An additional effect to consider, particularly at Mach numbers above about 2, is the change with angle of attack of the dynamic pressure in the wing flow field. This change involves an increase in dynamic pressure in the compression field below the wing and a decrease in dynamic pressure in the expansion field above the wing. Above $M \approx 2$ these pressure changes become large and, when coupled with the fact that the wing Mach lines become directed more nearly over the afterbody and tail, may outweigh the effects of forebody and wing-body vorticity. Under these conditions the high-wing configuration may have more favorable directional characteristics than the low-wing configuration since, with increasing angle of attack, the afterbody and tail would tend to move down into a high dynamic pressure field for the high-wing configuration whereas for the low-wing configuration the afterbody and tail would be subjected more to the low pressure field above the wing.

Vertical-tail pressure distribution.- The changes in tail contribution with wing position and with angle of attack for $M = 1.41$ and $M = 2.01$ (fig. 12) are the result of induced sidewash at the vertical tail. Some pressure measurements have been made on a vertical tail to determine the magnitude of these effects for various wing locations. Some of these results for $M = 1.41$ are shown in figures 13 and 14 for the same model used in obtaining the force results shown in figure 12. For a chordwise station near the root of the vertical tail at $\alpha = 0^\circ$ and $\beta = -5^\circ$ (fig. 13), the effect of the wing-induced sidewash is to increase the local angle of sideslip and the corresponding section loading for the low-wing configuration and to decrease the local angle of sideslip and corresponding section loading for the high-wing configuration. The complete span loading $c_y \frac{c_v}{\bar{c}_v}$ of the vertical tail for

$\beta = -5^\circ$ at $\alpha = 0^\circ$ and 15° is shown in figure 14. At $\alpha = 0^\circ$, the span loading is uniformly increased for the low wing and uniformly decreased for the high wing. At $\alpha = 15^\circ$, the same general changes occur although the wing effects are combined with body effects so that the changes in span loading are less uniform. The influence of the body flow at $\alpha = 15^\circ$ is apparent near the root of the tail where the section loading is less for the wing off than for the wing on in either the high or low positions.

The changes in tail contribution with angle of attack could also result from dynamic pressure changes rather than from sidewash angle changes. This is not likely, however, since some directional control investigation (for example, refs. 11 and 12) indicate that the effectiveness of a rudder or all-moving vertical tail is maintained even though the tail contribution to $C_{Y\beta}$ and $C_{n\beta}$ diminishes. This characteristic is indicative of a flow angle change at the tail rather than a dynamic pressure change.

Comparison of supersonic and subsonic sidewash effects.- The supersonic effects of the wing-induced sidewash at the vertical tail up to $M \approx 2$ are similar to those determined at low speeds. In figure 15, a comparison is made of the wing-position effects on the experimentally determined tail factor η_V for 45° sweptback-wing models at subsonic and supersonic speed ($M = 2.01$). The subsonic results (ref. 15) and the supersonic results (ref. 16) indicate essentially the same effects of wing height and angle of attack.

Effects of fuselage forebody on tail contribution.- The tail contribution to directional stability may be affected by a number of other things such as body cross-sectional shape, inlets, canopies, and horizontal tails. Some effects of fuselage forebody shape on the lateral and directional stability characteristics of a fuselage and fuselage-vertical-tail configuration at $M = 1.41$ are shown in figure 16. These fuselages have the same volume and cross-sectional-area distribution but differ in forebody cross-sectional shape - one having a circular shape, one having a vertically elliptical shape, and one having a horizontally elliptical shape. The results indicate a slight increase in tail contribution with increasing angle of attack for the horizontally elliptical forebody when compared to that for the circular forebody. With the vertically elliptical forebody, however, there is a considerable decrease in tail contribution with increasing angle of attack and the indications are that the tail contribution reverses above $\alpha \approx 12^\circ$.

The effect of a wing on the directional characteristics of a model with a forebody with protuberances simulating side inlets is shown in figure 17 for a 35° sweptback-wing configuration at $M = 1.61$. With the wing off, the induced flows around the body result in a rapid decrease in tail contribution and, in fact, indicate a reversal in tail contribution above $\alpha \approx 14^\circ$. With the wing installed in a semihigh position, the tail contribution is reduced slightly at low angles of attack, but with increasing angle of attack, the wing apparently shields the tail from some of the body flow field arising from the side protuberances and the decrease in tail contribution is much less than for the wing-off case.

Effects of horizontal tail.- The effects of a horizontal tail on the directional stability of two 45° sweptback-wing airplane models are shown

in figure 18 for a high- and low-tail position at $M = 1.41$. The addition of the horizontal tail at $\alpha = 0^\circ$ in either a high or low position causes an increase in directional stability. With increasing angle of attack, the increase provided by the low tail becomes smaller whereas the increase provided by the high tail becomes larger. The results shown in figure 18 are for the tail fixed at zero deflection, whereas in figure 19 deflections of the horizontal tail in a direction to provide longitudinal trim (trailing-edge up) at high angles of attack are shown to result in an increase in directional stability with the low tail and a decrease in directional stability with the high tail.

Effects of ventral fins.- A relatively simple way to augment the directional stability is through the use of ventral fins. The effects of ventral fins on the directional stability of two configurations at $M = 2.01$ are shown in figure 20. The single ventral fin mounted on the bottom center line of the fuselage adds an essentially constant increment to $C_{n\beta}$ through the angle-of-attack range for both configurations. The addition of four small cruciform fins to one of the configurations has little effect at $\alpha = 0^\circ$ but provides a substantial increase in $C_{n\beta}$ with increasing angle of attack. A further description of this type of fin arrangement may be found in reference 17.

Effects of afterbody modification.- Inasmuch as the fundamental problem in maintaining adequate directional stability for current high-speed aircraft stems from the large unstable moments of the fuselage, some consideration should be given to reducing this source of instability. This plan might involve reshaping of the fuselage or the use of multiple-body arrangements.

Some preliminary directional characteristics obtained for a body-alone configuration and a combination of body and vertical tail with two afterbody shapes at $M = 2.01$ are shown in figure 21. The basic body had a circular cross section and a length-diameter ratio of 11. The rearward 20 percent of the body was modified to have elliptical cross-sections with the major axis vertical. The maximum ratio of the major axis to the minor axis was 2.25 at the base of the body. Both bodies maintained the same cross-sectional-area distribution. The vertical tail for both bodies had the same total area to the body center line. Thus, the exposed area of the tail was less for the elliptical body than for the basic body.

The effect of the modified afterbody was substantially to reduce the instability of the body throughout the angle-of-attack range. With the vertical tail added, the gain in stability provided by the elliptical afterbody was about half that indicated for the body alone. However, with the elliptical afterbody, the exposed tail area is reduced about 25 percent and the aspect ratio of the tail is reduced.

The effects of the addition of a 45° sweptback wing in both a high and low position for the body with the vertically elliptical afterbody both with and without a vertical tail are shown in figure 22 for $M = 2.01$. The effects of wing position for the model with the elliptical afterbody are qualitatively the same as for a conventional afterbody. (See fig. 12, for example.) That is, with increasing angle of attack, the addition of the high wing reduced the instability of the wing-body combination but also reduced the tail contribution; whereas, the addition of the low wing increased the instability of the wing-body combination but had little effect on the tail contribution. Quantitatively, however, in comparison to results for the conventional afterbody, the effects of wing position with the elliptical afterbody were more pronounced for the tail-off configurations and less pronounced for the tail-on contribution. Therefore, unlike the model with a conventional afterbody (fig. 12), the model with the vertically elliptical afterbody (fig. 22) has higher directional stability and lower tail loads with the high wing than with the low wing.

Effects of small-span forebody fins.- Some preliminary results have been obtained at $M = 2.01$ to determine the effects of small-span forebody fins, called strakes, extending over the forward 30 percent of the body, on the directional stability characteristics of a model with a 60° delta wing (fig. 23). The strakes, which were mounted on the horizontal center line, had a span of 0.1 of the body diameter. The effects of the strakes were to reduce the directional instability of the wing-body combination at higher angles of attack as well as to increase the tail contribution slightly so that a substantial increase in directional stability was realized. These results are in general agreement with results obtained for a 45° sweptback-wing configuration at high subsonic speeds (ref. 18) and at $M = 1.41$ (unpublished).

Characteristics of multiple-body configurations.- Low-speed tests of a multiple-body configuration (ref. 19) indicate that the directional stability improved considerably over that for a conventional configuration, primarily because of a decrease in the instability of the wing-body combination with increasing angle of attack. This decrease results in part from the elimination of the center afterbody that is generally adversely affected by the vorticity induced by the forebody and the wing-body juncture. In addition, the two outer bodies provide a stabilizing increment in $C_{n\beta}$ with increasing angle of attack because of the forward location of the center of gravity with respect to the outer bodies. Similar characteristics might be expected at supersonic speeds.

In addition, multiple-body configurations (such as that shown in fig. 24) may offer some relief to the inertia coupling problem and may also provide horizontal-tail locations suitable from the standpoint of pitch-up.

CONCLUDING REMARKS

A survey was made of the problems introduced by the increased longitudinal stability and reduced directional stability of aircraft operating in the low supersonic speed range. The increased longitudinal stability results in high drags due to trimming and in limited control for maneuvering.

The untrimmed pitching moments can be reduced and hence the control requirements can be alleviated to some extent through the use of fuselage camber. The use of canard configurations offers promise of reducing the drag due to trimming and increasing the controllability.

The primary problem of concern in the case of directional stability at supersonic speeds is the reduction in lift-curve slope of the vertical tail coupled with the large unstable yawing moment of the fuselage. The vertical-tail contribution is shown to be affected by many factors including the wing position, the fuselage shape, and the horizontal-tail position. The directional stability can be increased, particularly at high angles of attack, by such devices as ventral fins and forebody strakes. In addition, indications are that the directional stability might be improved through modifications to the fuselage afterbody.

Langley Aeronautical Laboratory,
National Advisory Committee for Aeronautics,
Langley Field, Va., May 3, 1957.

REFERENCES

1. Spearman, M. Leroy, and Henderson, Arthur, Jr.: Some Effects of Aircraft Configuration on Static Longitudinal and Directional Stability Characteristics at Supersonic Mach Numbers Below 3. NACA RM L55L15a, 1956.
2. Sevier, John R., Jr.: Investigation of the Effects of Body Camber and Body Indentation on the Longitudinal Characteristics of a 60° Delta-Wing--Body Combination at a Mach Number of 1.61. NACA RM L56A03, 1956.
3. Spearman, M. Leroy, and Driver, Cornelius: Investigation of Aerodynamic Characteristics in Pitch and Sideslip of a 45° Sweptback-Wing Airplane Model With Various Vertical Locations of Wing and Horizontal Tail - Static Longitudinal Stability and Control, $M = 2.01$. NACA RM L55L06, 1956.
4. Palazzo, Edward B., and Spearman, M. Leroy: Static Longitudinal and Lateral Stability and Control Characteristics of a Model of a 35° Swept-Wing Airplane at a Mach Number of 1.41. NACA RM L54G08, 1955.
5. Spearman, M. Leroy, Driver, Cornelius, and Robinson, Ross B.: Aerodynamic Characteristics of Various Configurations of a Model of a 45° Swept-Wing Airplane at a Mach Number of 2.01. NACA RM L54J08, 1955.
6. Smith, Willard G.: Wind-Tunnel Investigation at Subsonic and Supersonic Speeds of a Fighter Model Employing a Low-Aspect-Ratio Unswept Wing and a Horizontal Tail Mounted Well Above the Wing Plane - Longitudinal Stability and Control. NACA RM A54D05, 1954.
7. Spearman, M. Leroy, and Palazzo, Edward B.: An Investigation of a Supersonic Aircraft Configuration Having a Tapered Wing With Circular-Arc Sections and 40° Sweepback - Aerodynamic Characteristics of the Configuration Equipped With a Canard Control Surface at a Mach Number of 1.89. NACA RM L54H19, 1954.
8. Driver, Cornelius: Longitudinal and Lateral Stability and Control Characteristics of Two Canard Airplane Configurations at Mach Numbers of 1.41 and 2.01. NACA RM L56L19, 1957.
9. Bates, William R.: Low-Speed Static Longitudinal Stability Characteristics of a Canard Model Having a 60° Triangular Wing and Horizontal Tail. NACA RM L9H17, 1949.

10. Johnson, Joseph L., Jr.: A Study of the Use of Various High-Lift Devices on the Horizontal Tail of a Canard Airplane Model as a Means of Increasing the Allowable Center-of-Gravity Travel. NACA RM L52K18a, 1953.
11. Spearman, M. Leroy, and Robinson, Ross B.: Static Lateral Stability and Control Characteristics of a Model of a 45° Swept-Wing Fighter Airplane With Various Vertical Tails at Mach Numbers of 1.41, 1.61, and 2.01. NACA RM L56D05, 1956.
12. Spearman, M. Leroy: Static Lateral and Directional Stability and Effective Sidewash Characteristics of a Model of a 35° Swept-Wing Airplane*at a Mach Number of 1.61. NACA RM L56E23, 1956.
13. Spearman, M. Leroy, and Driver, Cornelius: Longitudinal and Lateral Stability Characteristics of a Low-Aspect-Ratio Unswept-Wing Airplane Model at Mach Numbers of 1.82 and 2.01. NACA RM L56H06, 1957.
14. Nielsen, Jack N., Kaattari, George E., and Anastasio, Robert F.: A Method for Calculating the Lift and Center of Pressure of Wing-Body-Tail Combinations at Subsonic, Transonic, and Supersonic Speeds. NACA RM A53G08, 1953.
15. Goodman, Alex: Effects of Wing Position and Horizontal-Tail Position on the Static Stability Characteristics of Models With Unswept and 45° Sweptback Surfaces With Some Reference to Mutual Interference. NACA TN 2504, 1951.
16. Spearman, M. Leroy, Driver, Cornelius, and Hughes, William C.: Investigation of Aerodynamic Characteristics in Pitch and Sideslip of a 45° Sweptback-Wing Airplane Model With Various Vertical Locations of Wing and Horizontal Tail - Basic-Data Presentation, $M = 2.01$. NACA RM L54L06, 1955.
17. Spearman, M. Leroy, Robinson, Ross B., and Driver, Cornelius: The Effects of the Addition of Small Fuselage-Mounted Fins on the Static Directional Stability Characteristics of a Model of a 45° Swept-Wing Airplane at Angles of Attack Up to 15.3° at a Mach Number of 2.01. NACA RM L56D16a, 1956.
18. Sleeman, William C., Jr.: Investigation at High Subsonic Speeds of the Effects of Various Fuselage Forebody Fins on the Directional and Longitudinal Stability of a Complete Model Having a 45° Sweptback Wing. NACA RM L56J25, 1957.
19. Fournier, Paul G.: Low-Speed Investigation of Static Longitudinal and Lateral Stability Characteristics of an Airplane Configuration With a Highly Tapered Wing and With Several Body and Tail Arrangements. NACA RM L57A08, 1957.

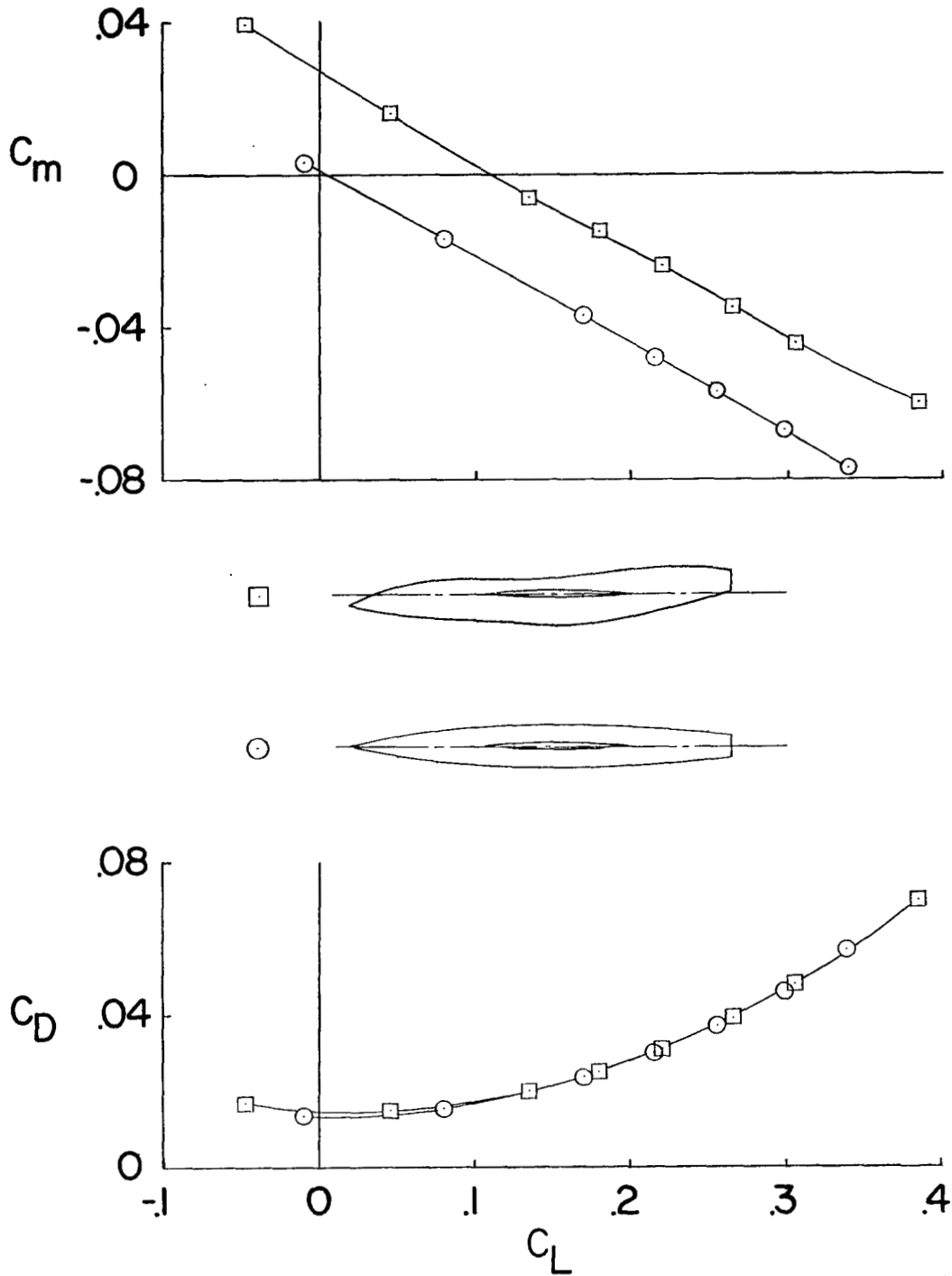


Figure 1.- Effect of fuselage camber on longitudinal stability characteristics at $M = 1.61$.

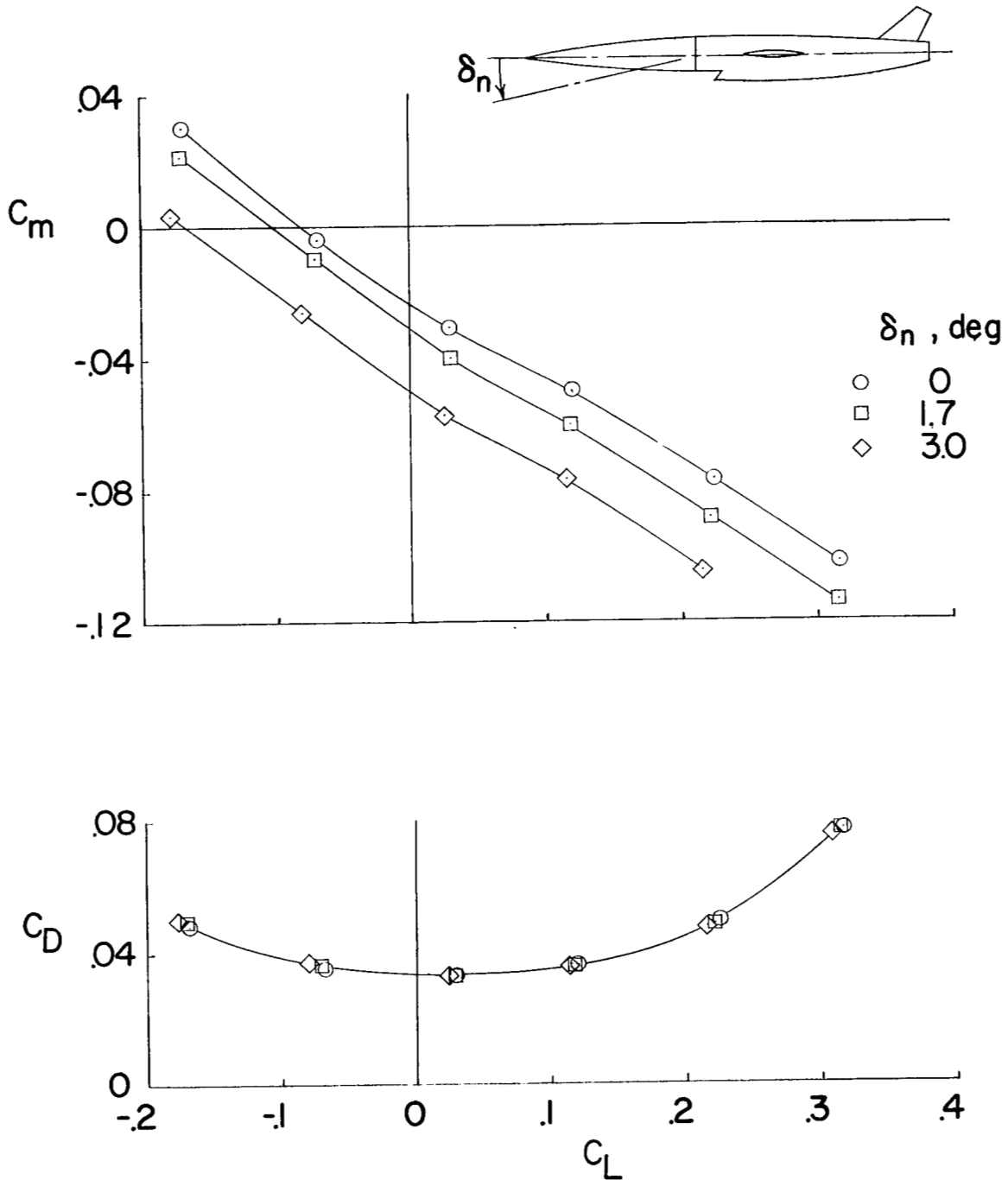


Figure 2.- Effect of fuselage-forebody deflection on longitudinal stability characteristics at $M = 2.01$.

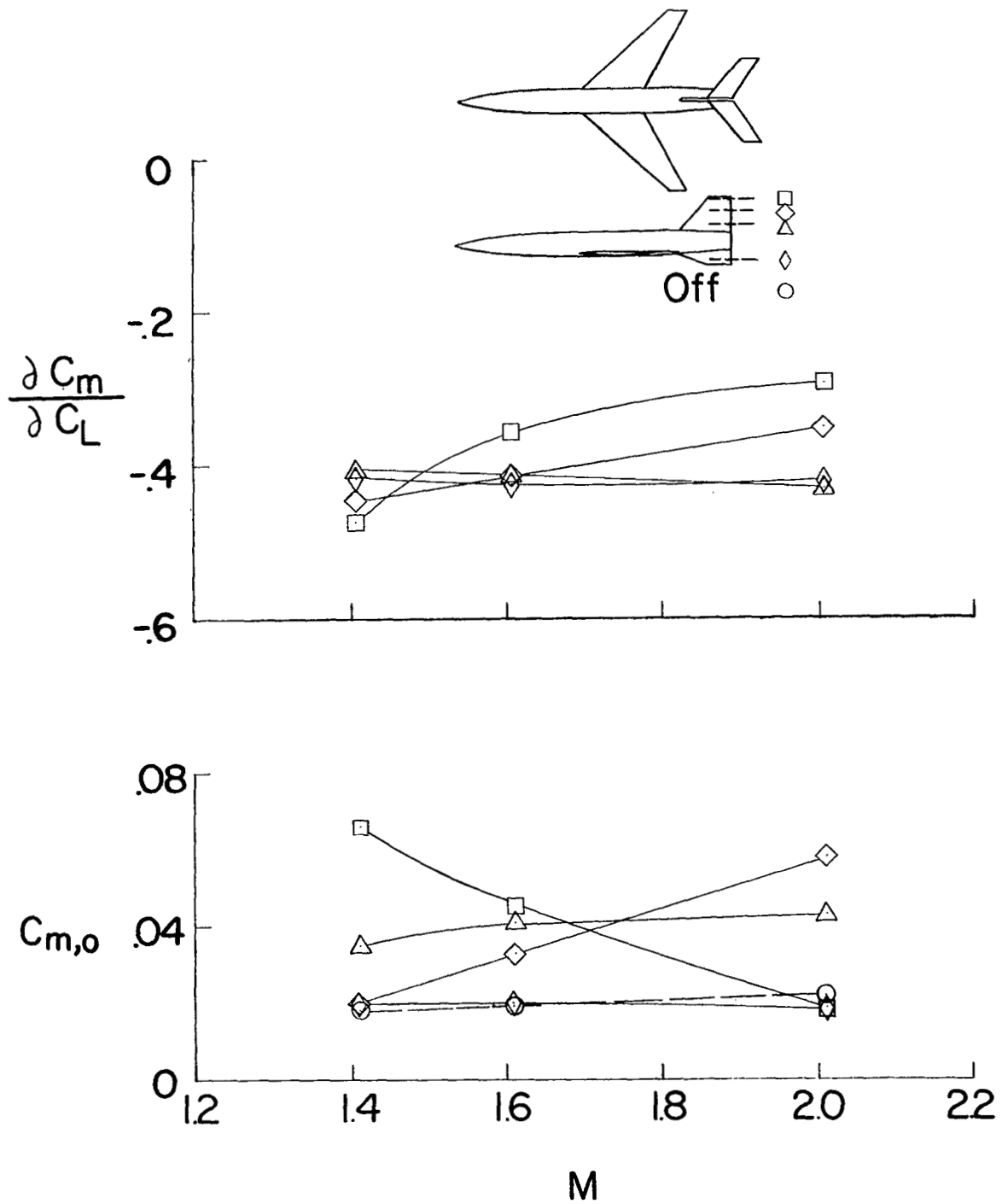


Figure 3.- Effect of horizontal-tail position on variation of $C_{m,0}$ and $\frac{\partial C_m}{\partial C_L}$ with Mach number.

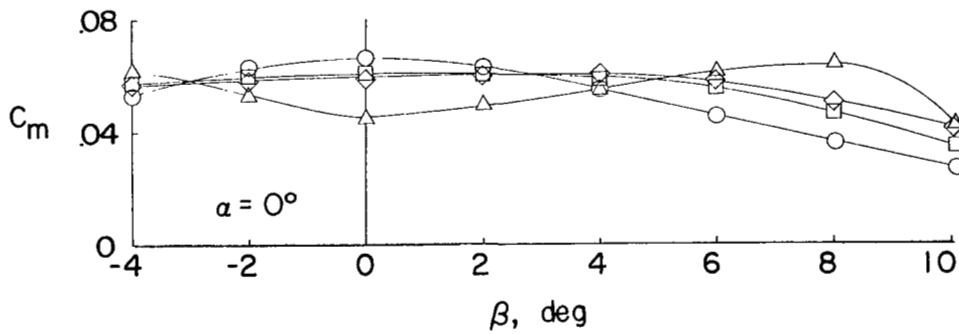
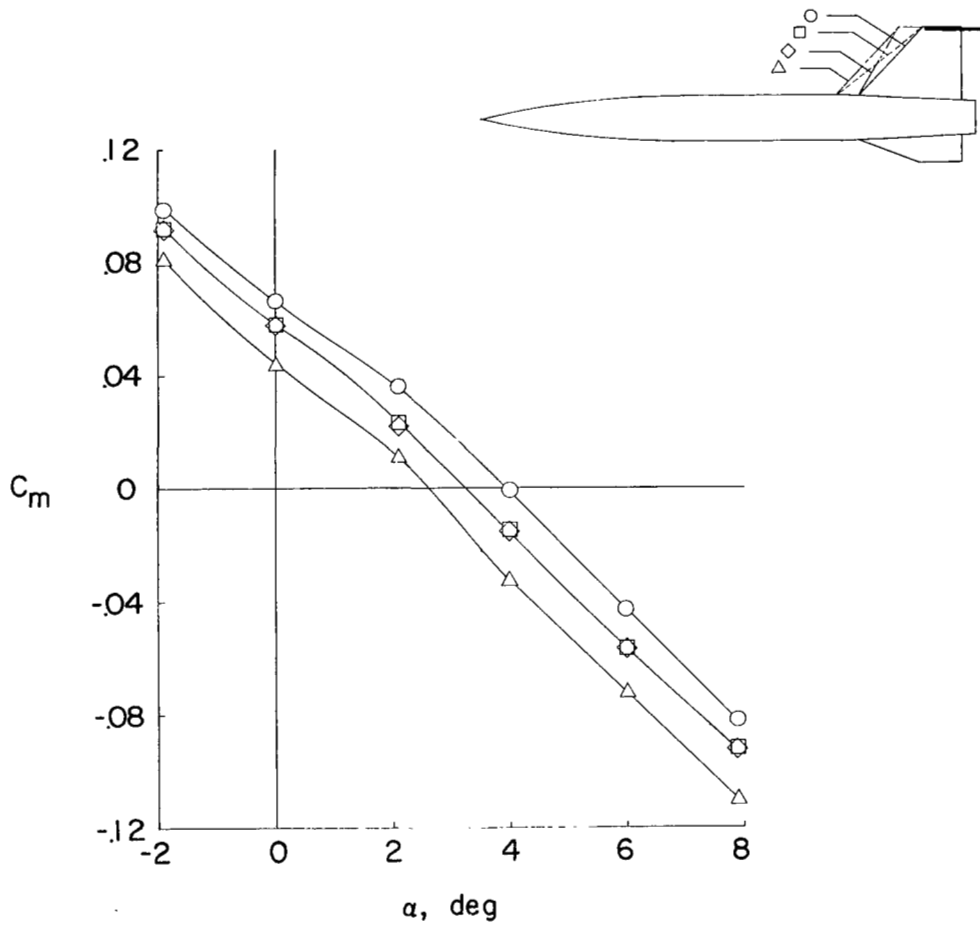


Figure 4.- Effect of vertical-tail plan form on pitching-moment characteristics of BVH configuration at $M = 1.41$.

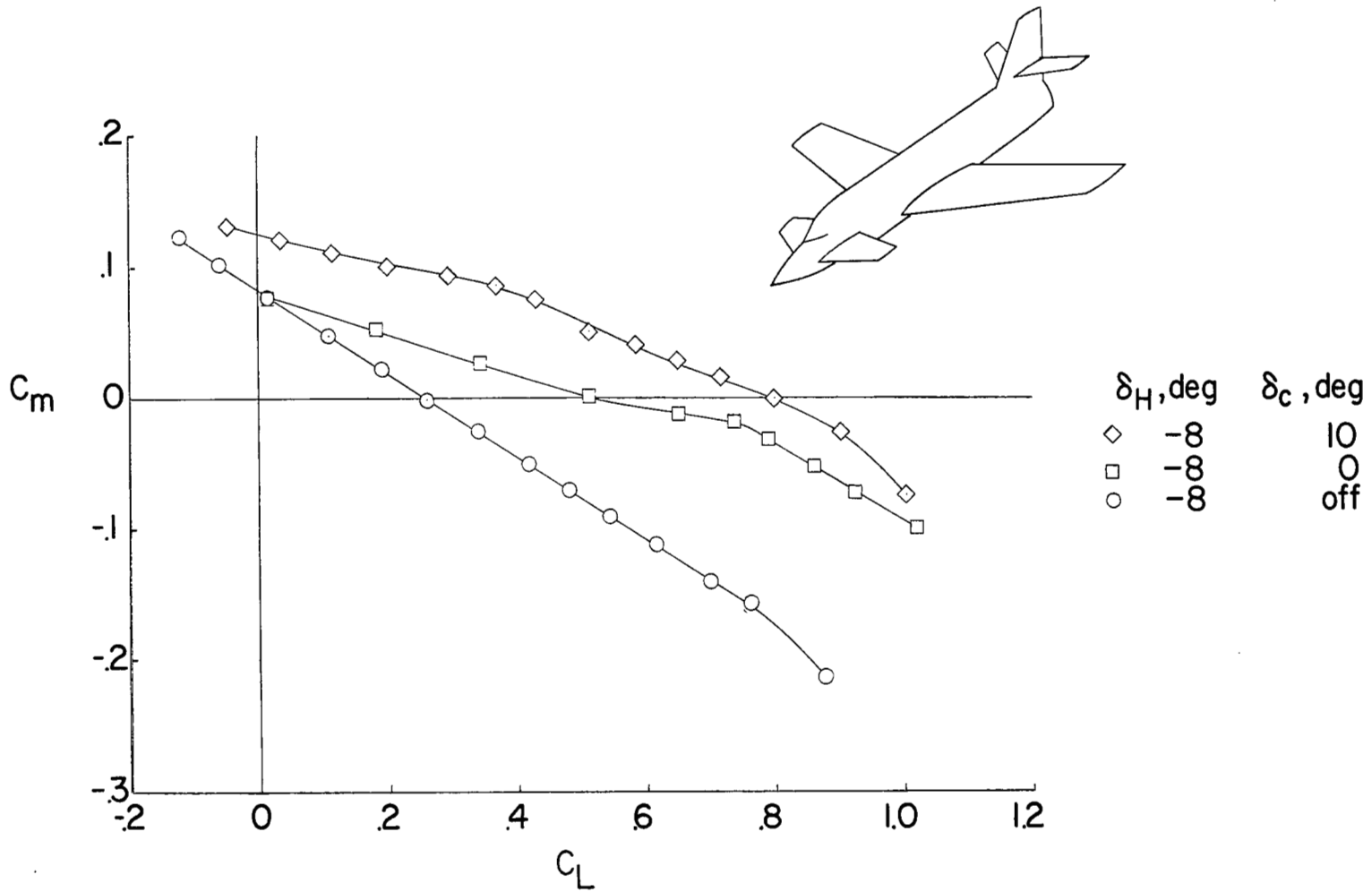


Figure 5.- Effects of auxiliary canard on longitudinal stability and control characteristics of 40° sweptback-wing airplane at $M = 1.89$.

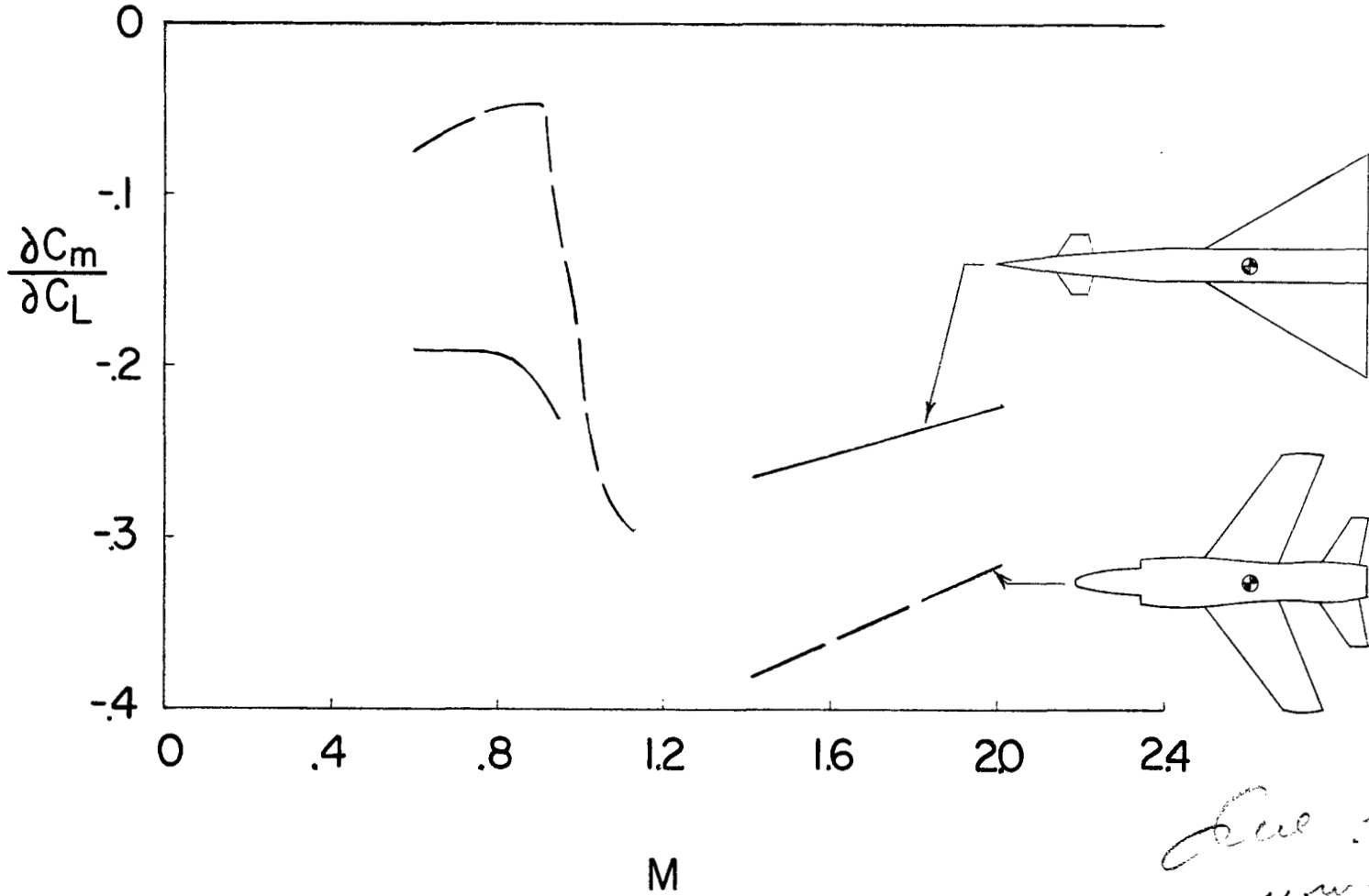


Figure 6.- Variation of longitudinal-stability parameter with Mach number for canard and tail-rearward configurations.

See p. 10
wing

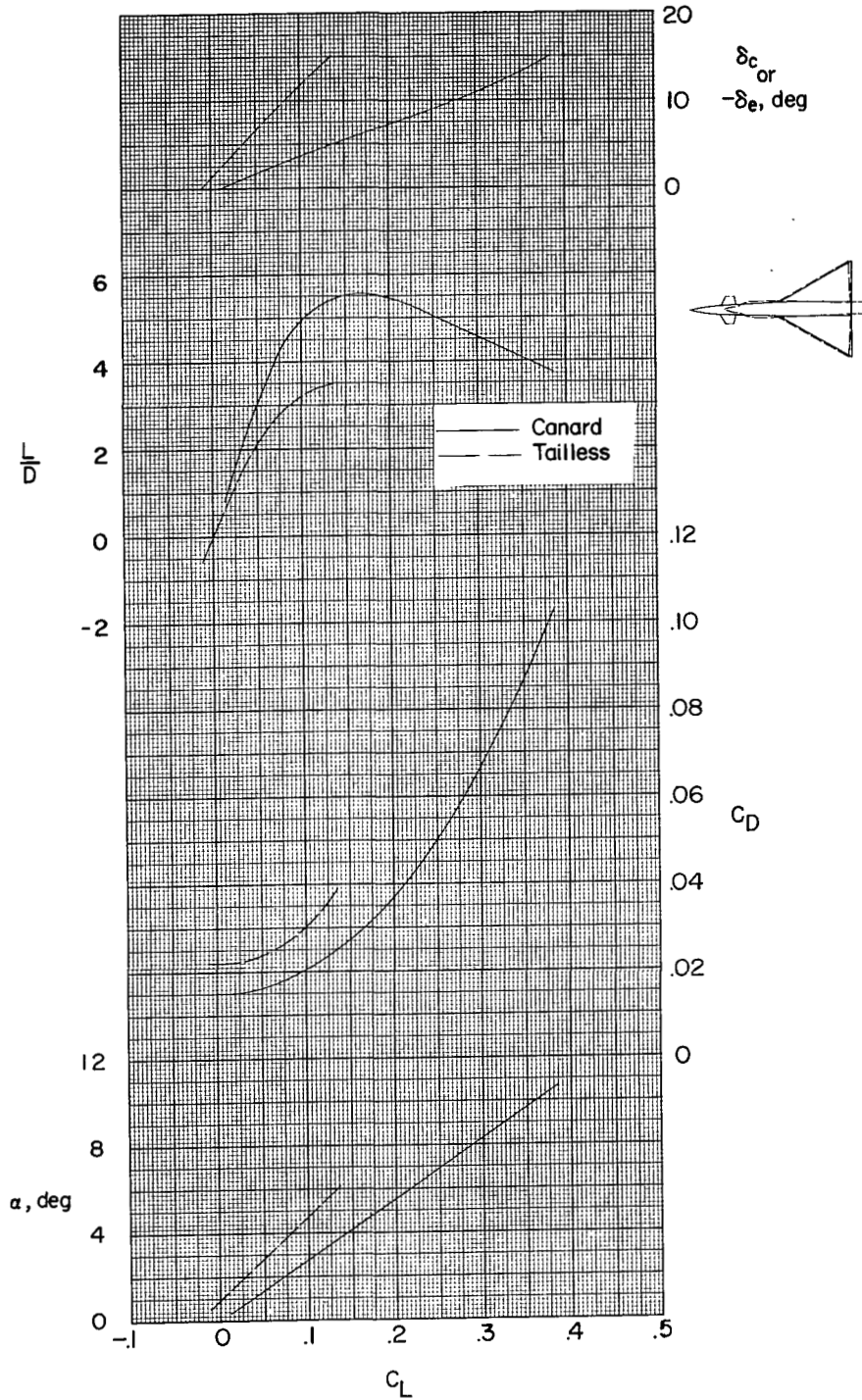


Figure 7.- Trimmed longitudinal stability characteristics for canard and tailless delta-wing configurations at $M = 2.01$.

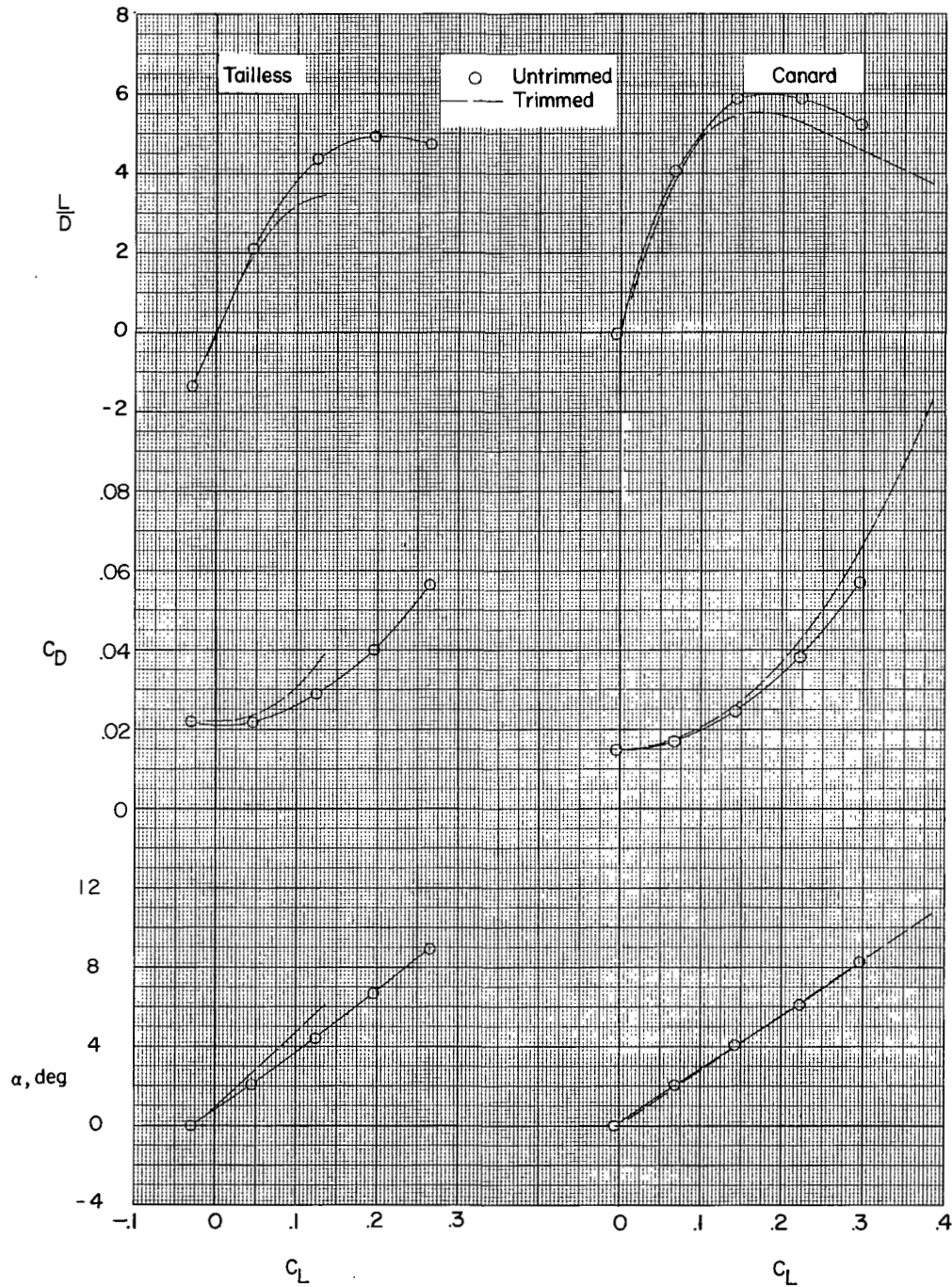


Figure 8.- Comparison of trimmed and untrimmed longitudinal stability characteristics for canard and tailless delta-wing configurations at $M = 2.01$.

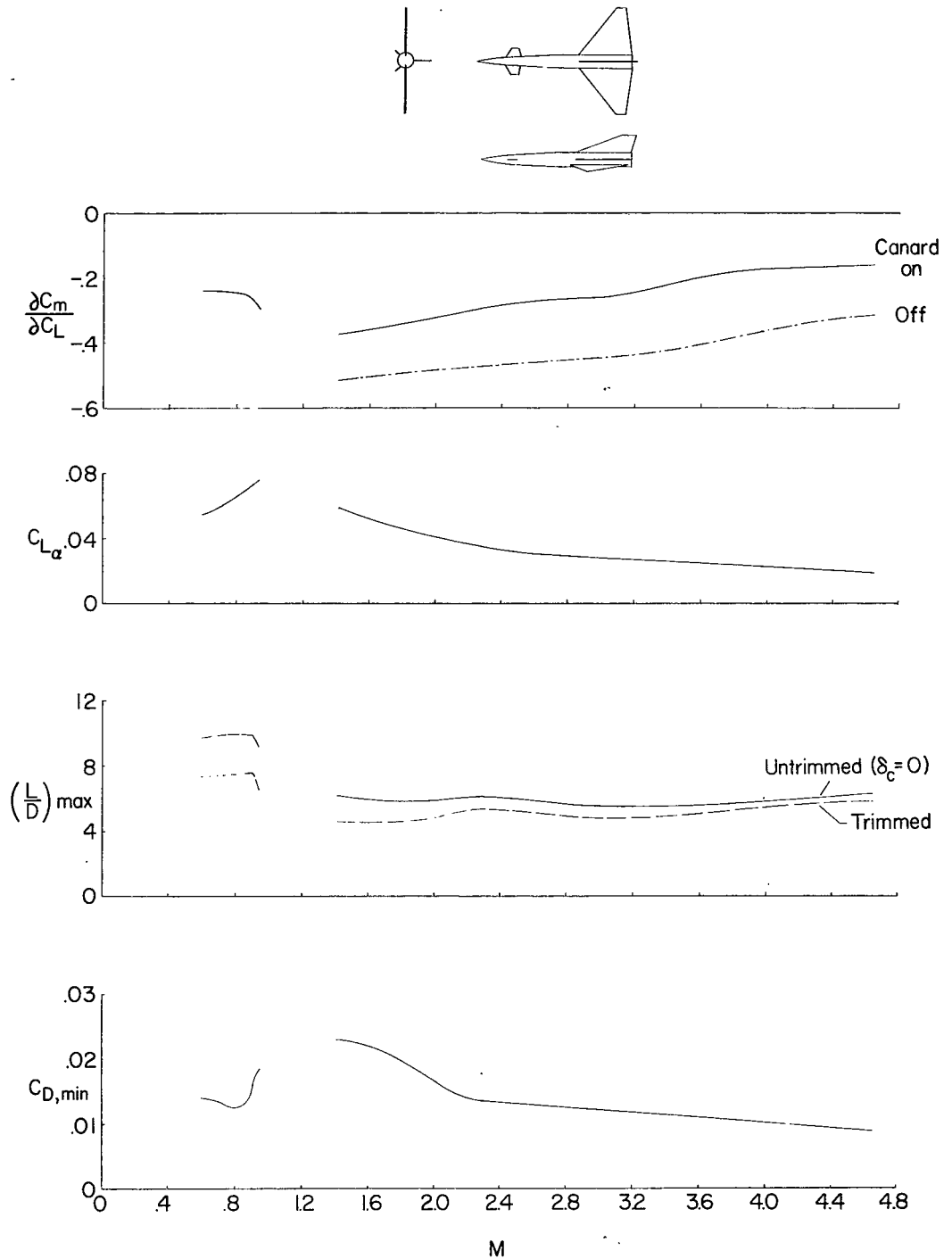


Figure 9.- Variation of longitudinal-stability characteristics with Mach number for canard configuration.

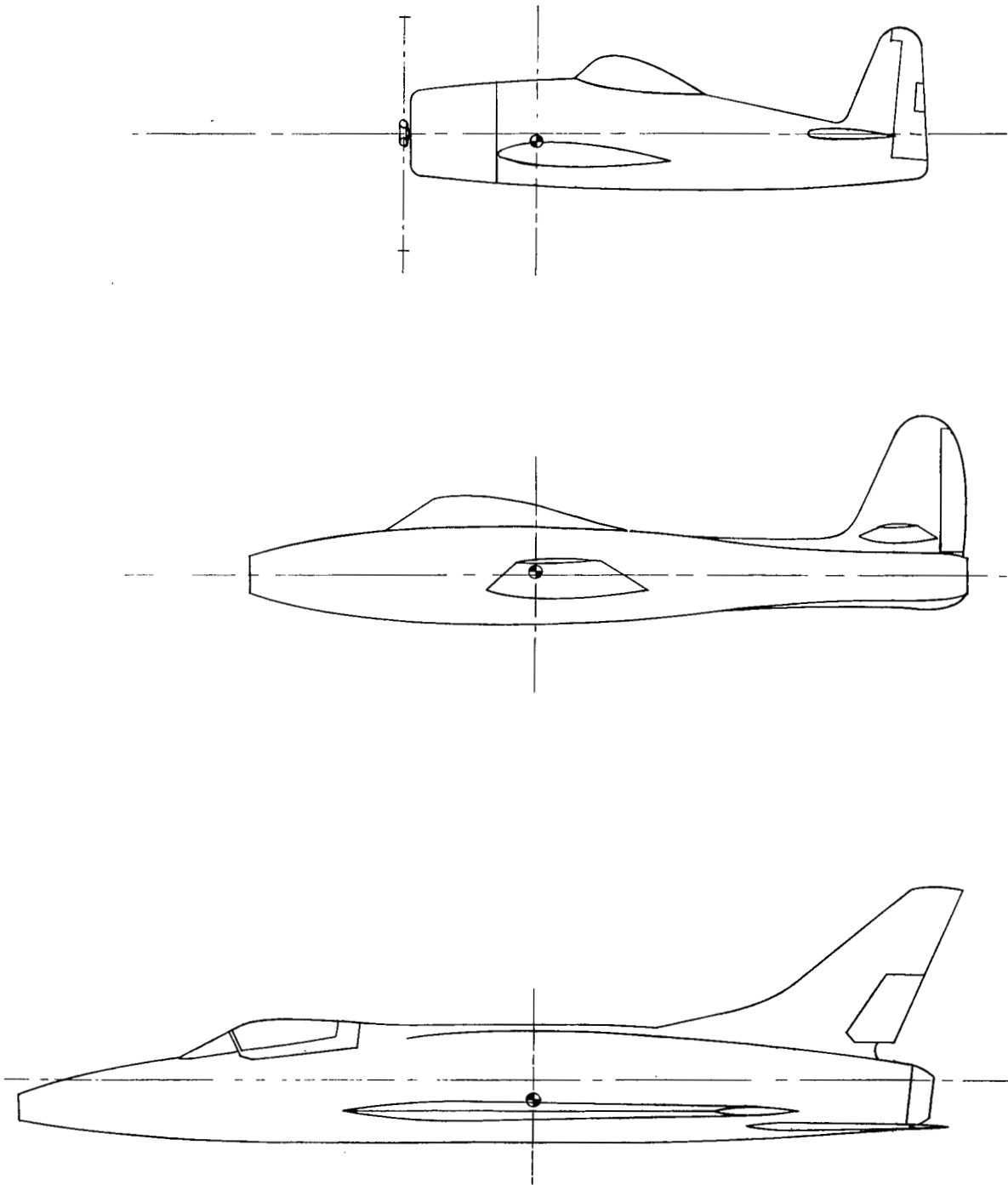


Figure 10.- Design trends of single-engine, single-place fighter airplanes.

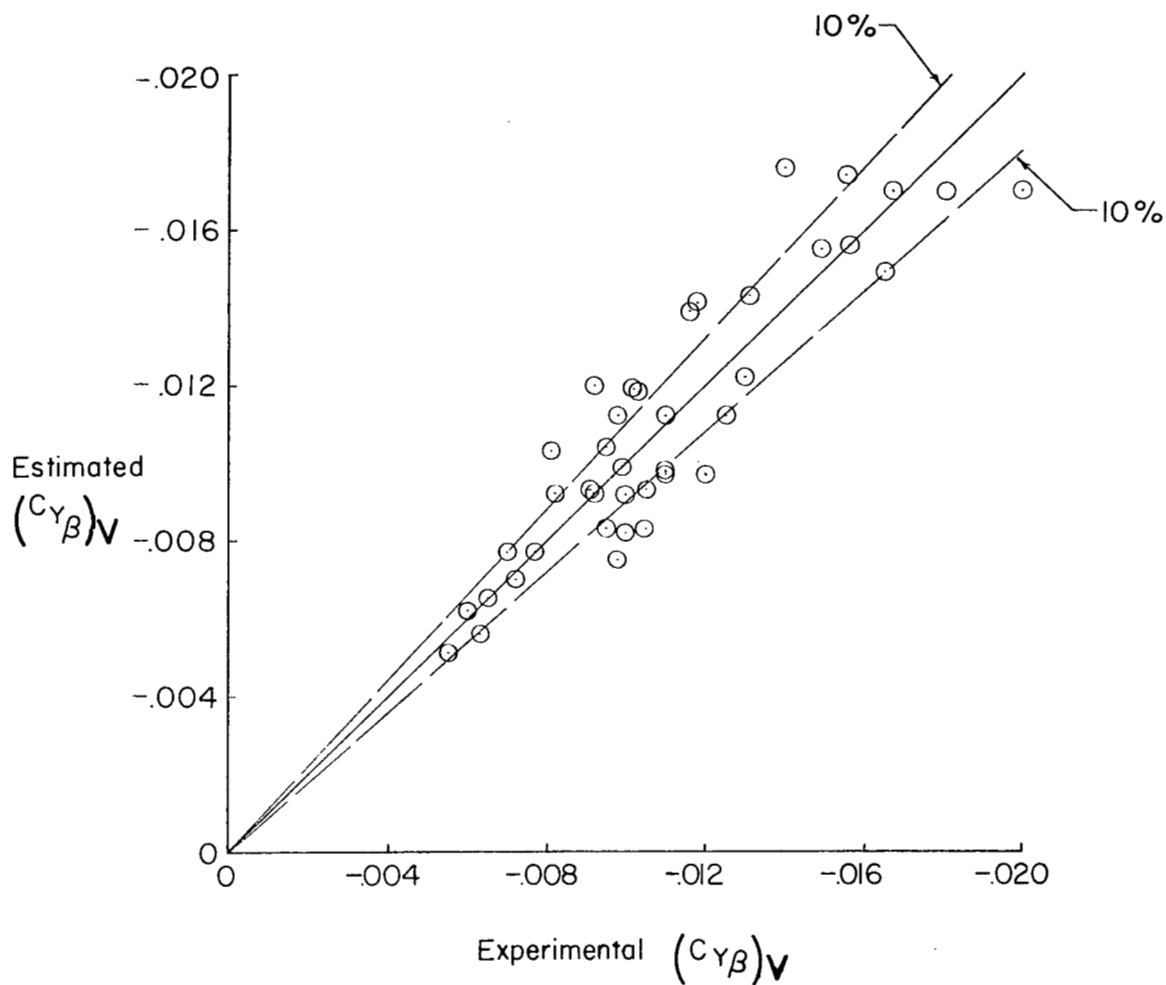
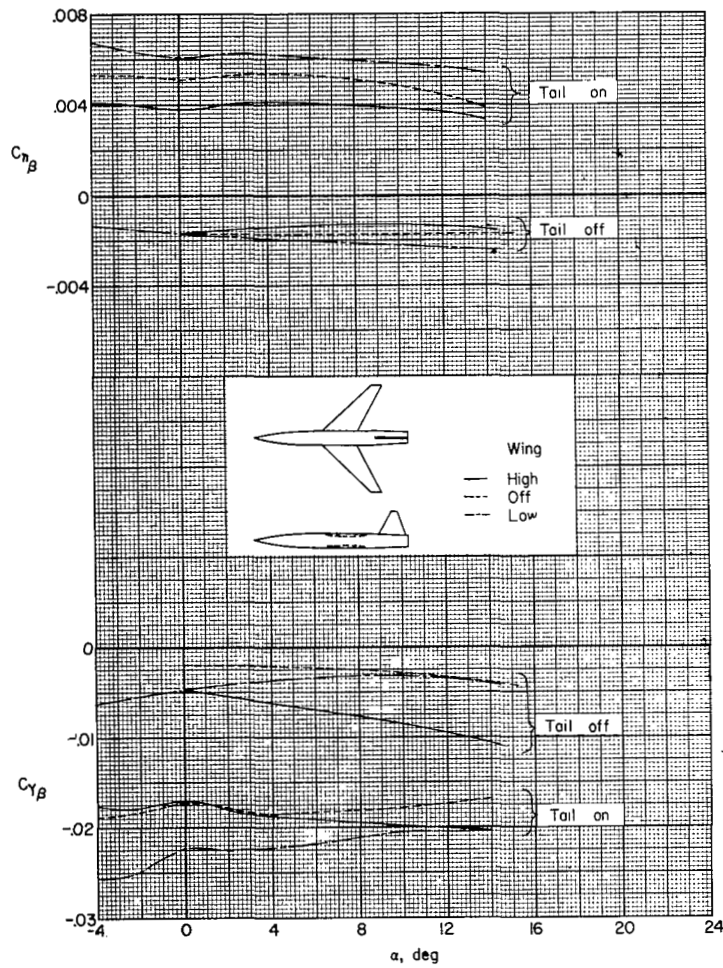
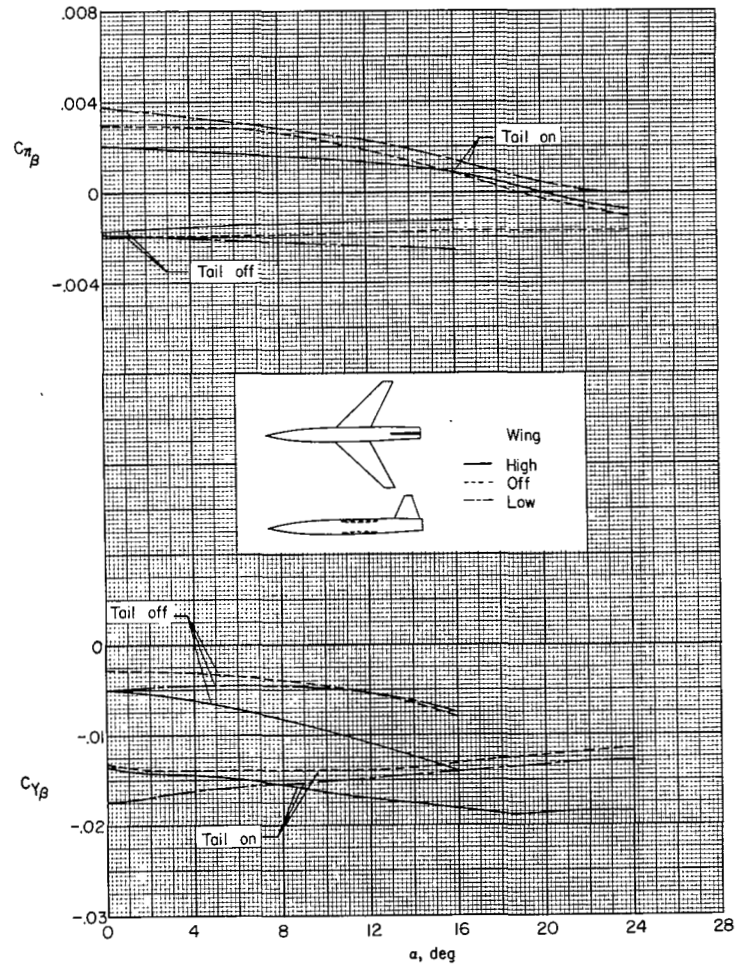


Figure 11.- Correlation of estimated and experimental values of vertical-tail contribution to $C_{Y\beta}$. $M = 1.4$ to 2.0 ; $\alpha = 0^\circ$.



(a) $M = 1.41$.



(b) $M = 2.01$.

Figure 12.- Effect of wing position on directional stability characteristics of a 45° sweptback-wing model.

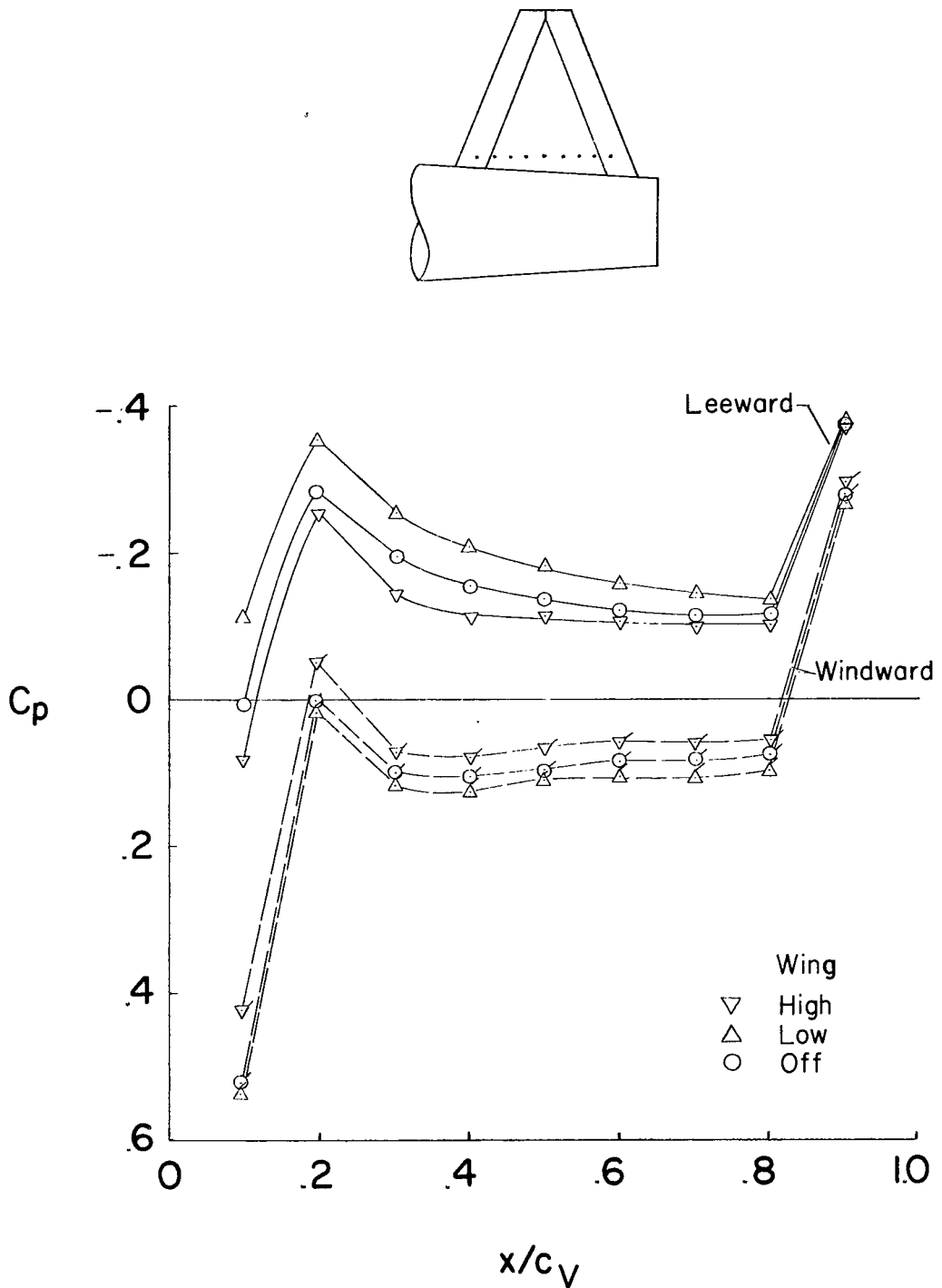


Figure 13.- Effect of wing position on vertical-tail section pressure distribution of a 45° sweptback-wing model. $\alpha = 0^\circ$; $\beta = -5^\circ$; $M = 1.41$.

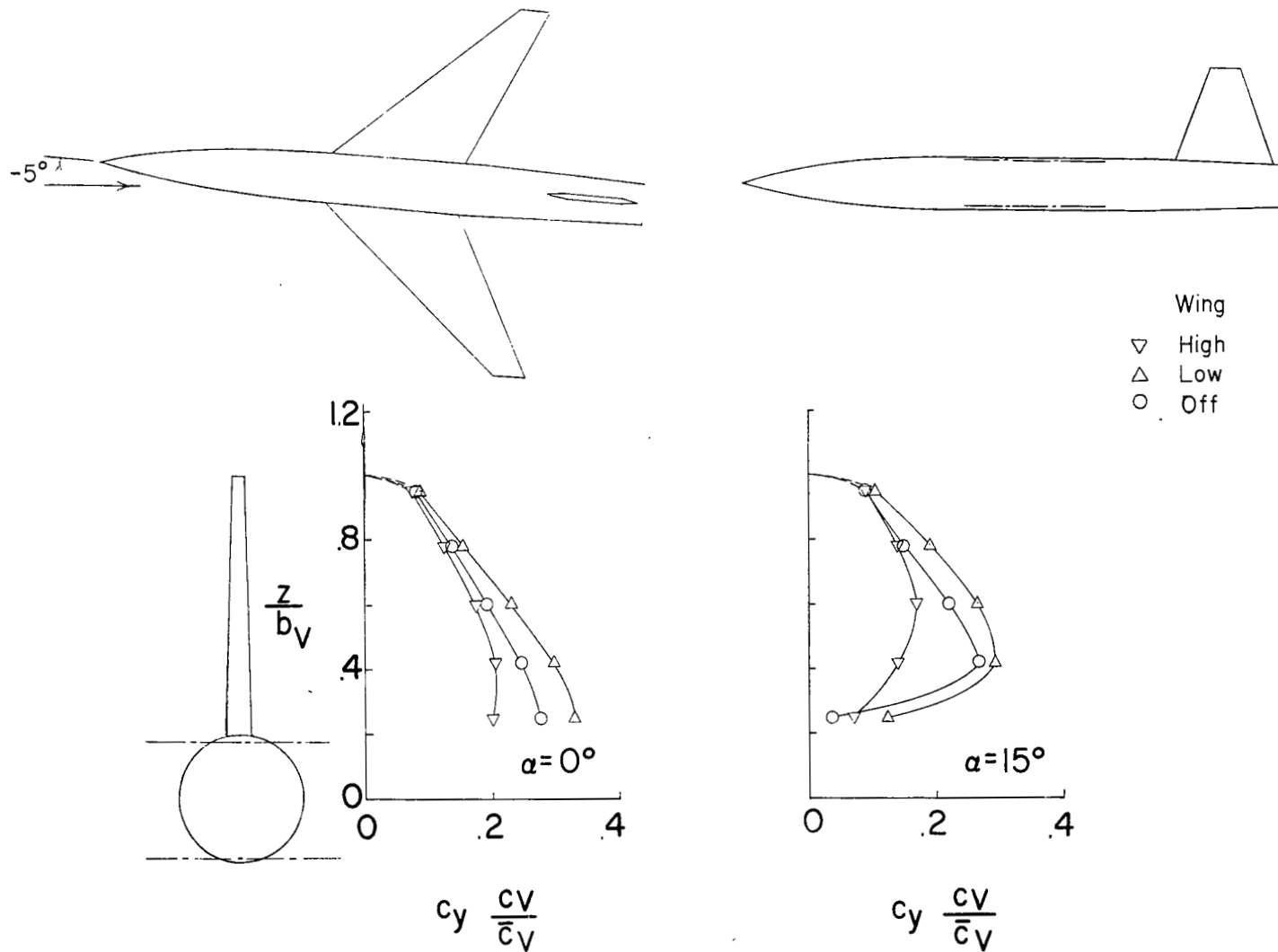


Figure 14.- Effects of wing position on vertical-tail span-load distribution of a 45° sweptback-wing model. $\beta = -5^\circ$; $M = 1.41$.

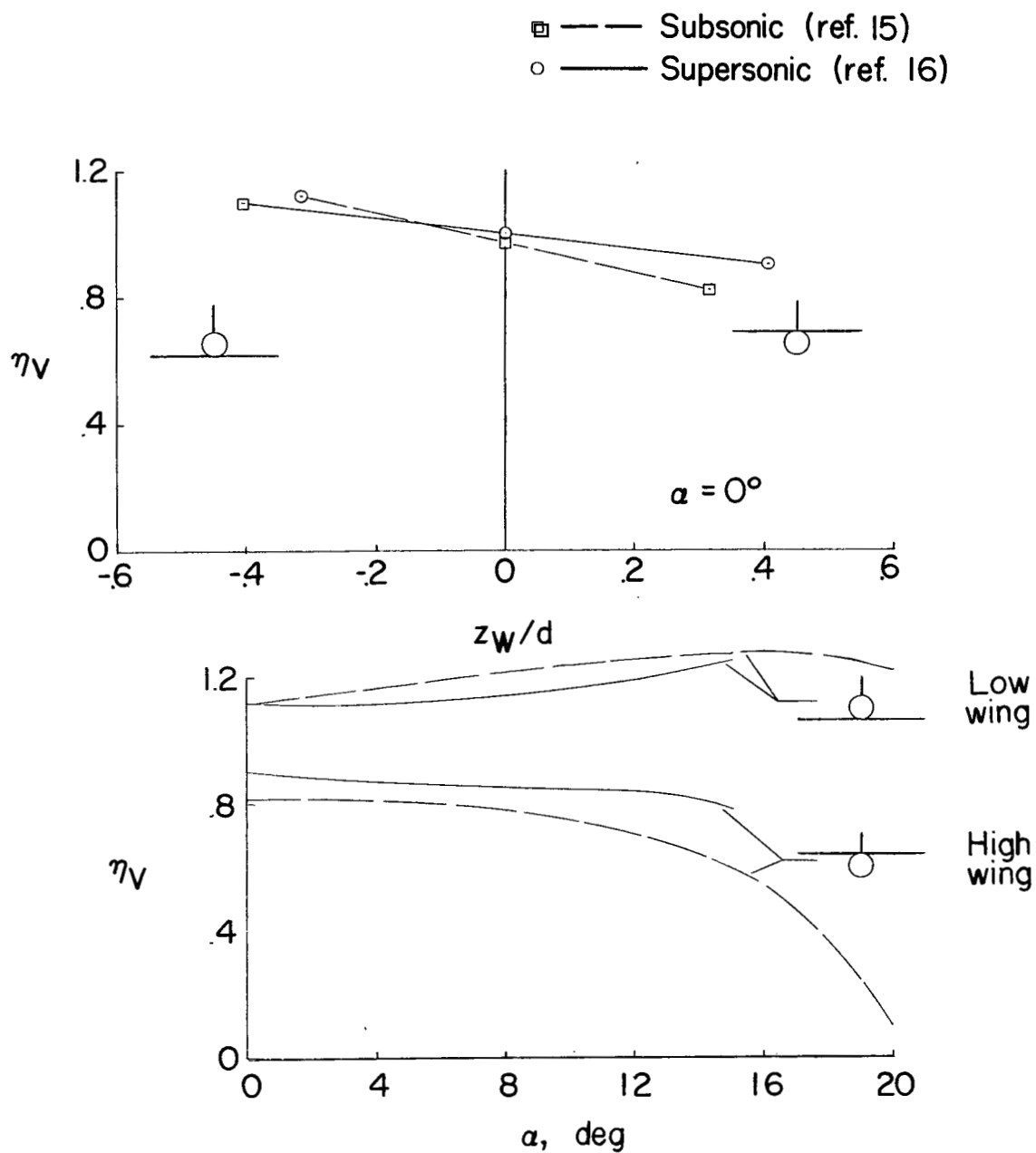


Figure 15.- Effect of wing position on vertical-tail efficiency of a 45° swept-wing model at subsonic and supersonic speeds.

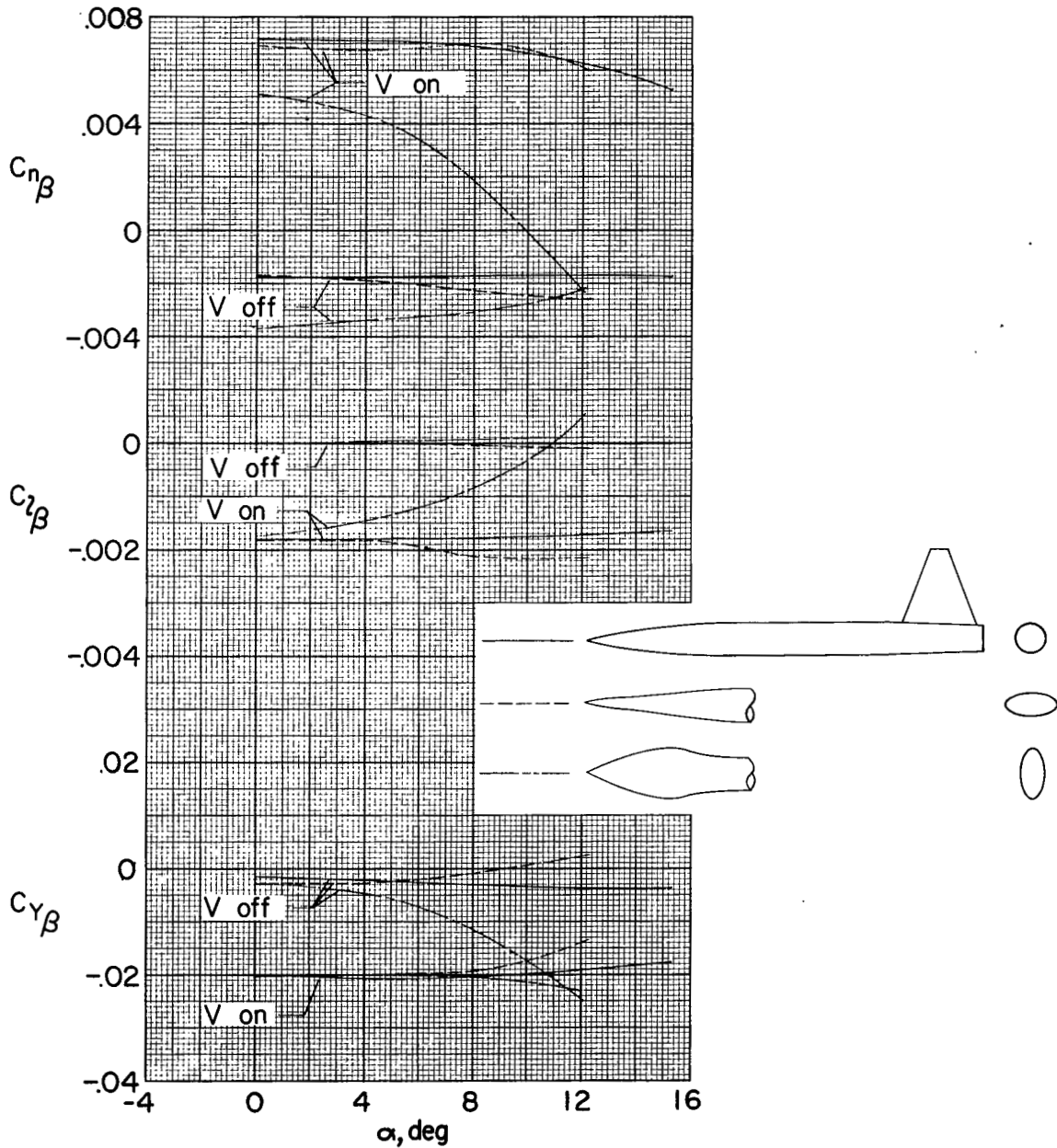


Figure 16.- Effect of forebody shape on vertical-tail contribution at $M = 1.41$.

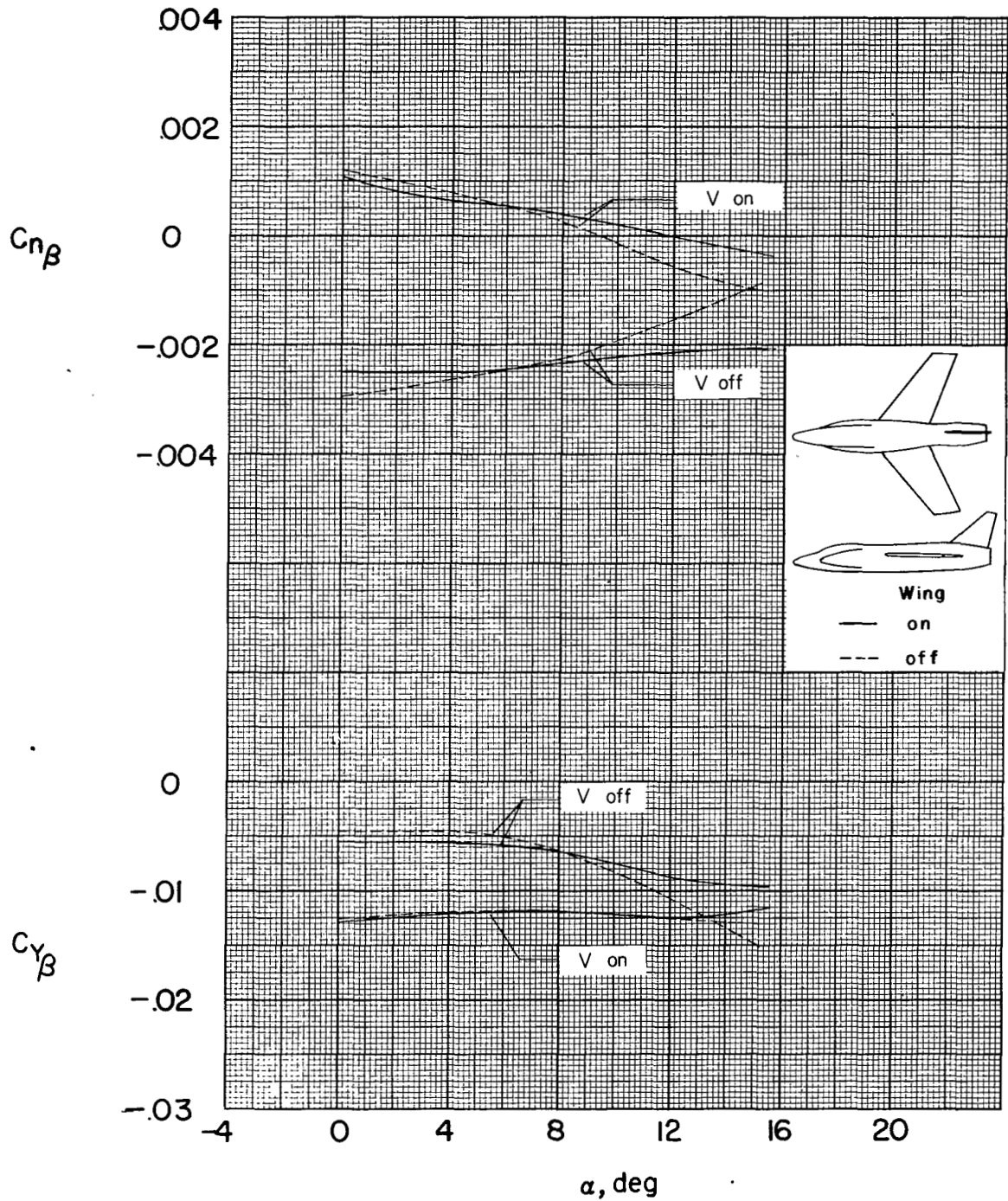


Figure 17.- Effect of wing on vertical-tail contribution of a 35° sweptback-wing configuration at $M = 1.61$.

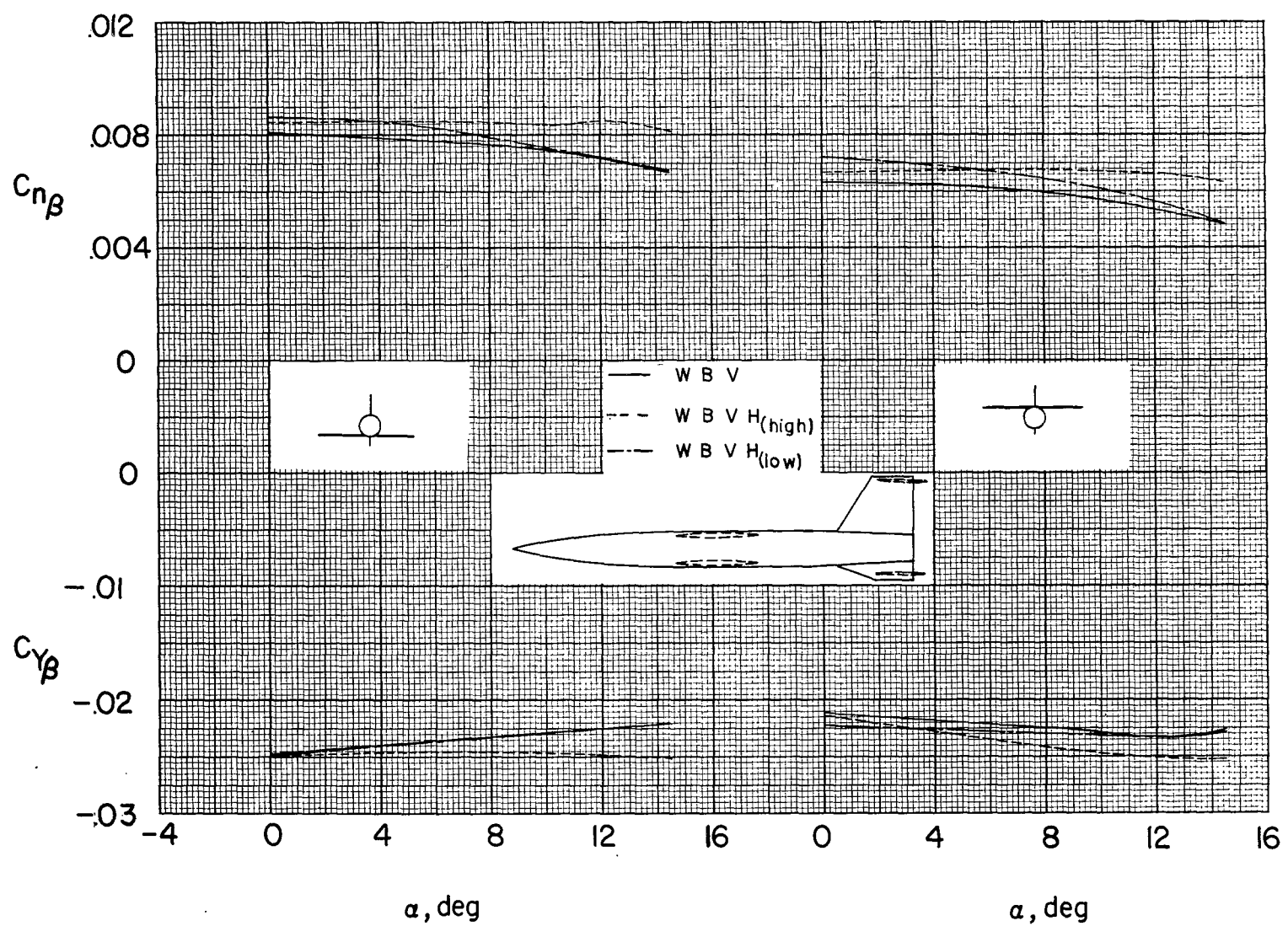


Figure 18.- Effect of horizontal tail on direction-stability characteristics of a 45° sweptback-wing model at $M = 1.41$.

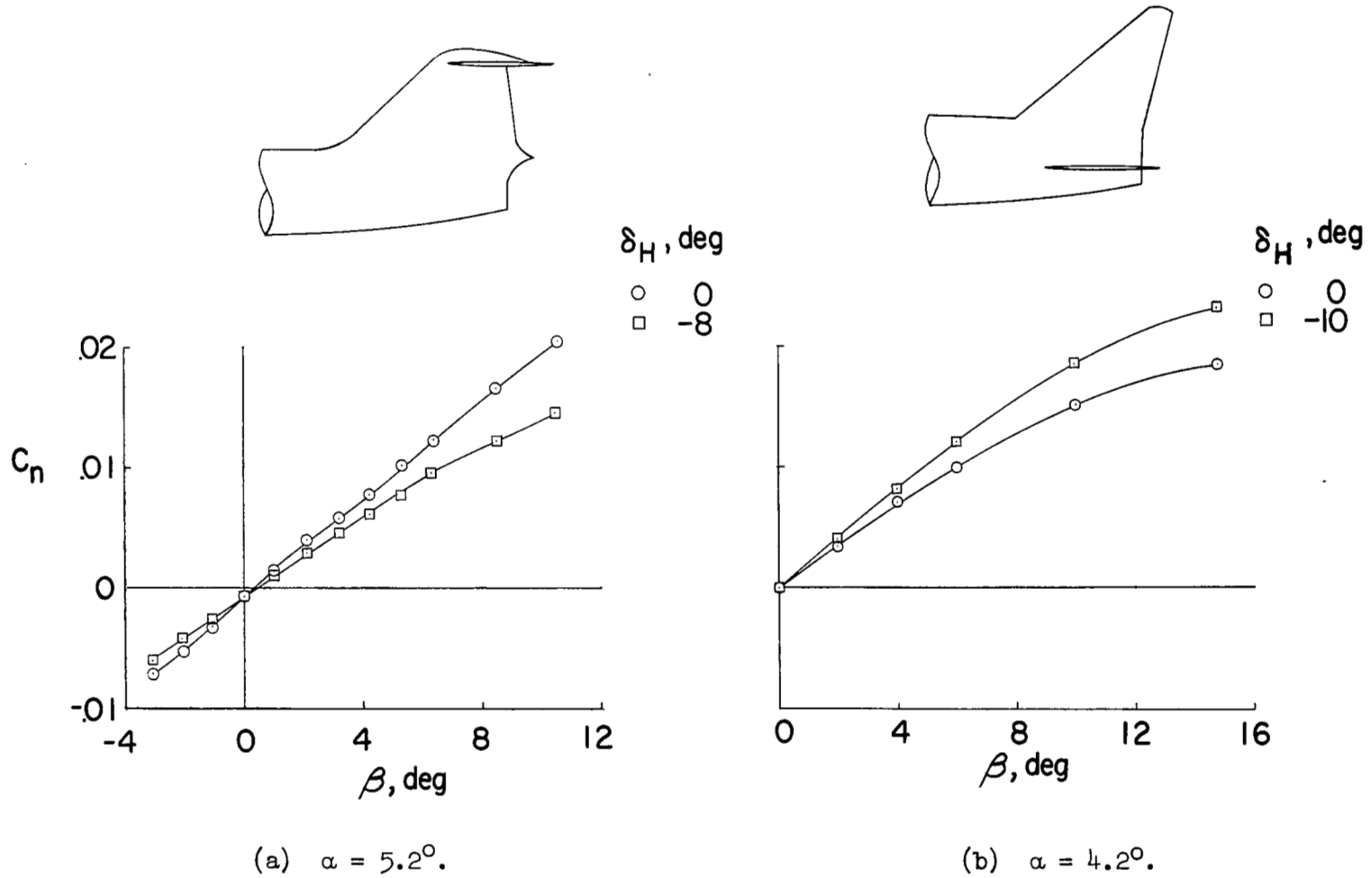


Figure 19.- Effects of horizontal-tail deflection on directional-stability characteristics for high and low horizontal tails at $M = 2.01$.

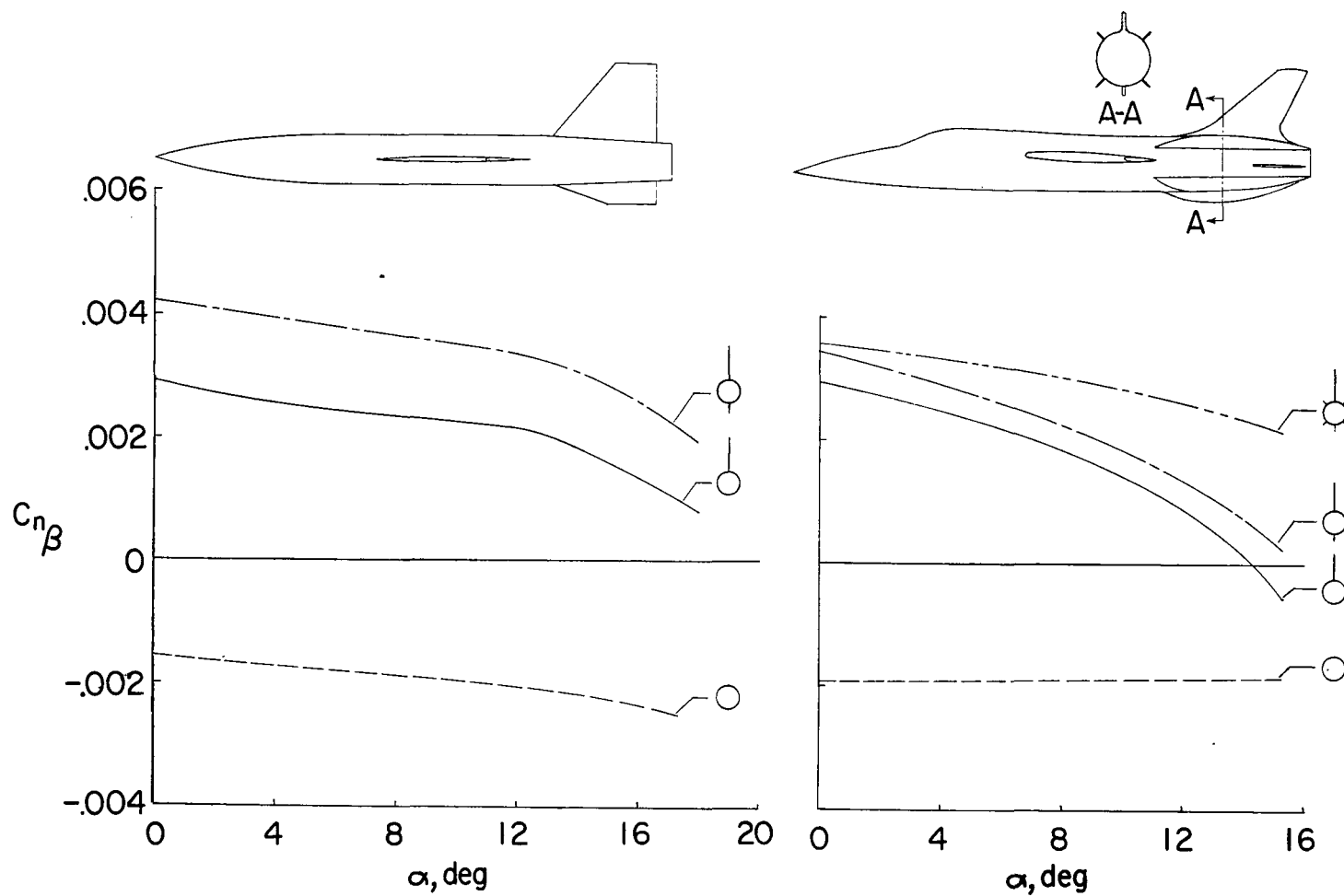


Figure 20.- Effects of ventral fins on directional-stability parameter at $M = 2.01$.

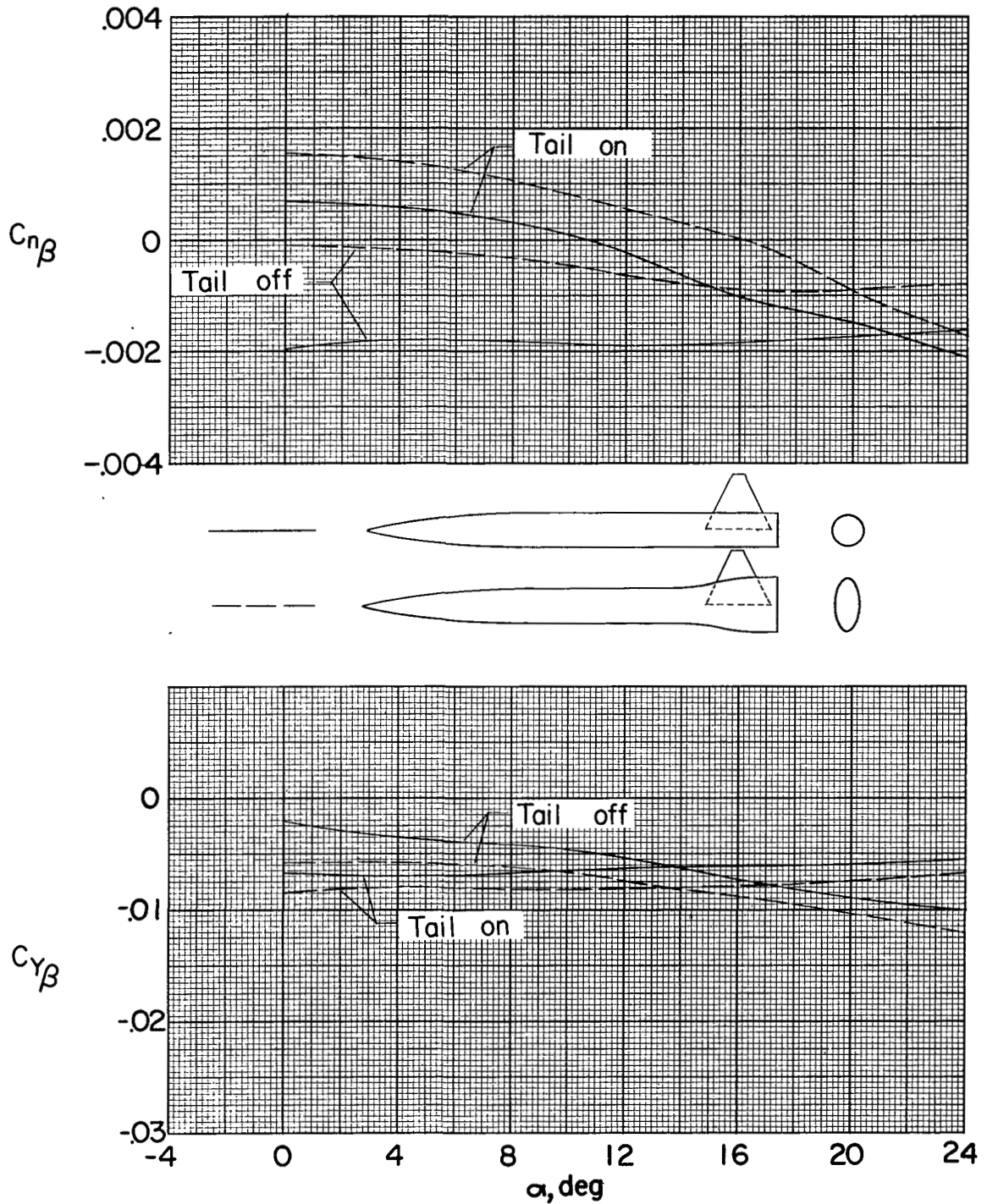


Figure 21.- Effect of afterbody shape on directional-stability characteristics at $M = 2.01$.

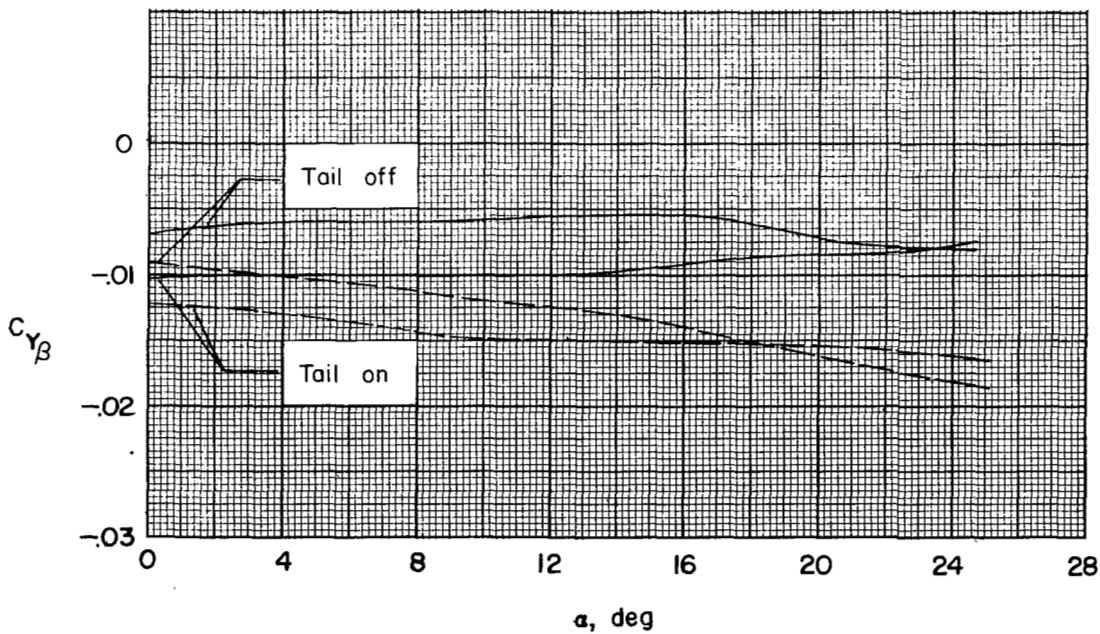
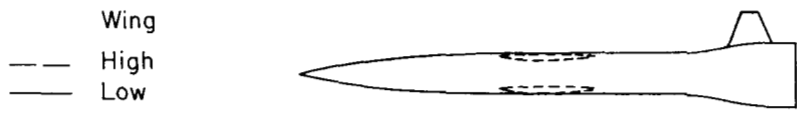
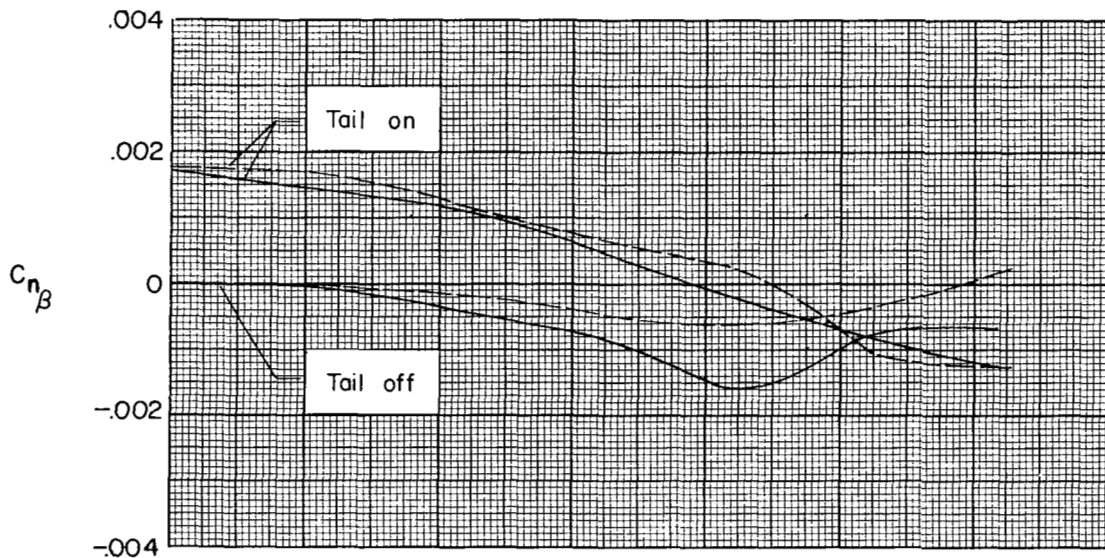


Figure 22.- Effect of wing position on directional characteristics of configuration with vertically elliptical afterbody at $M = 2.01$.

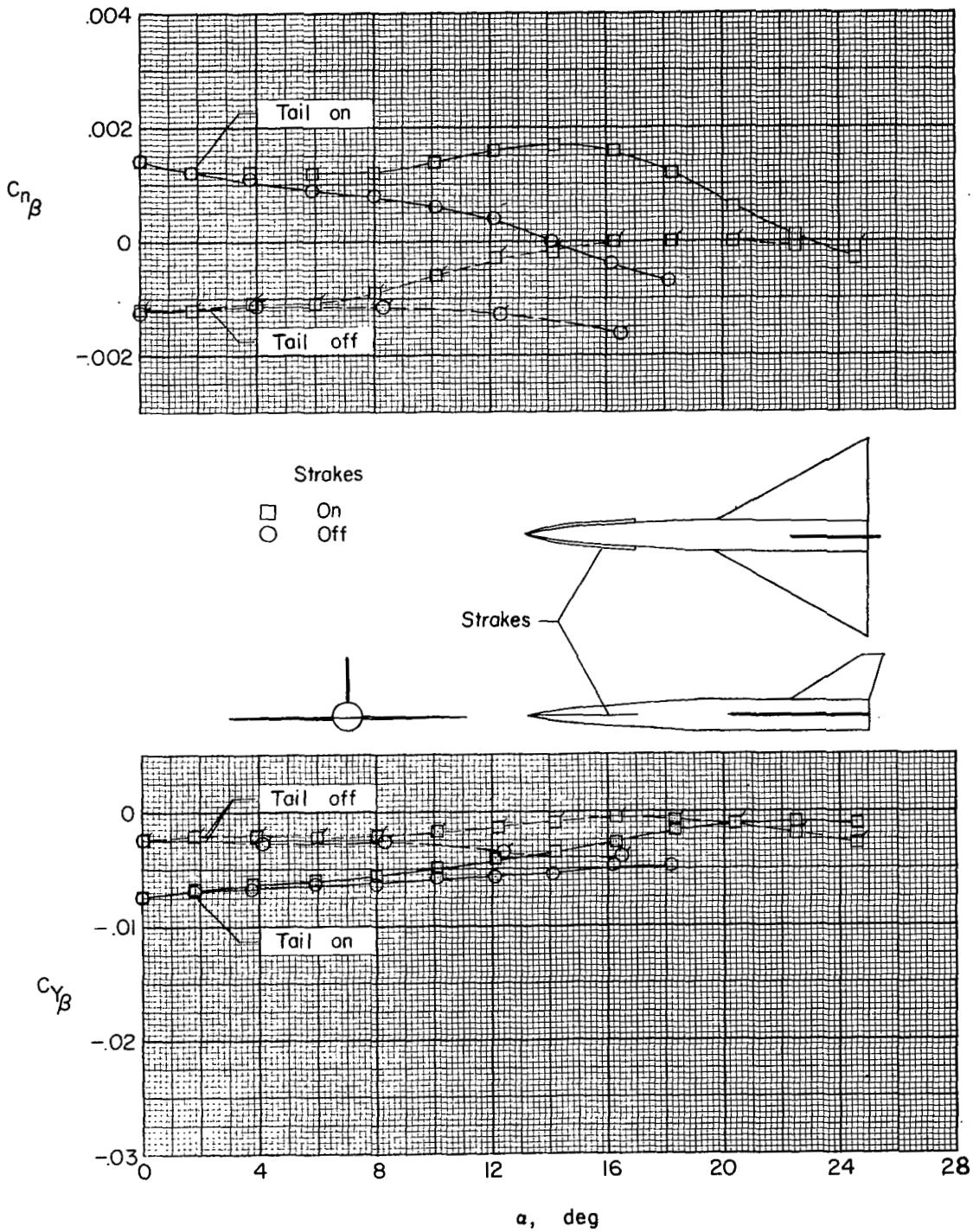
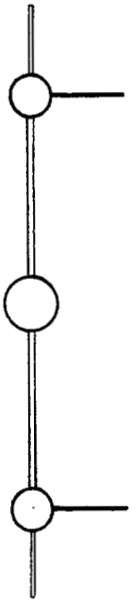
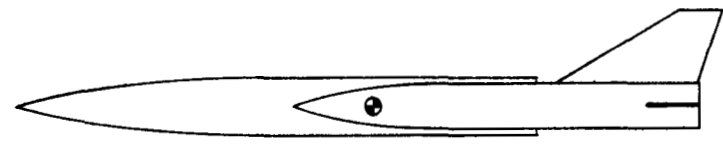
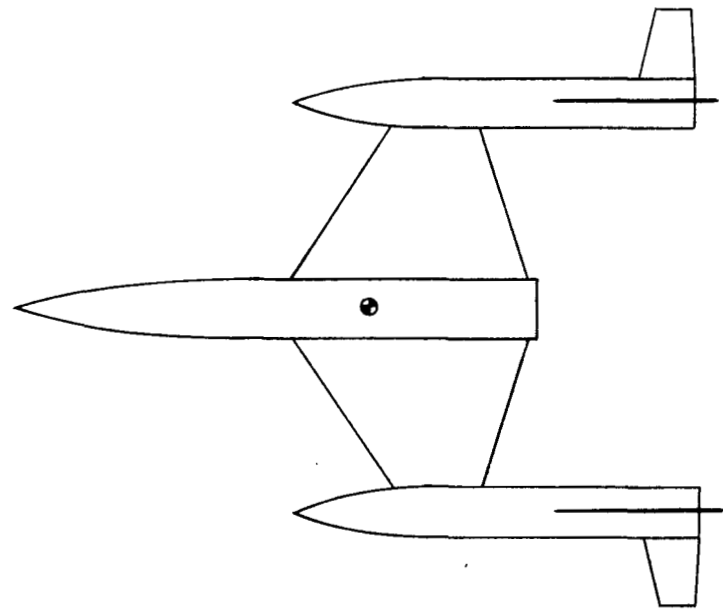


Figure 23.- Effect of forebody strakes on the directional stability characteristics of a 60° delta-wing configuration at M = 2.01.



HAYES TARGET DISK
 TmT-1
 EGlin AIR MUSEUM

Figure 24.- Multiple-body configuration.

